

Cy 2



STATISTICAL PREDICTION OF MAXIMUM TIME-VARIANT INLET DISTORTION LEVELS

J. L. Jacocks and K. R. Kneile
ARO, Inc.

PROPULSION WIND TUNNEL FACILITY
ARNOLD ENGINEERING DEVELOPMENT CENTER
AIR FORCE SYSTEMS COMMAND
ARNOLD AIR FORCE STATION, TENNESSEE 37389

January 1975

Final Report for Period July 1, 1972 — June 30, 1974

Approved for public release; distribution unlimited.

Prepared for

DIRECTORATE OF TECHNOLOGY
ARNOLD ENGINEERING DEVELOPMENT CENTER
ARNOLD AIR FORCE STATION, TENNESSEE 37389

NOTICES

When U. S. Government drawings specifications, or other data are used for any purpose other than a definitely related Government procurement operation, the Government thereby incurs no responsibility nor any obligation whatsoever, and the fact that the Government may have formulated, furnished, or in any way supplied the said drawings, specifications, or other data, is not to be regarded by implication or otherwise, or in any manner licensing the holder or any other person or corporation, or conveying any rights or permission to manufacture, use, or sell any patented invention that may in any way be related thereto.

Qualified users may obtain copies of this report from the Defense Documentation Center.

References to named commercial products in this report are not to be considered in any sense as an endorsement of the product by the United States Air Force or the Government.

This report has been reviewed by the Information Office (OI) and is releasable to the National Technical Information Service (NTIS). At NTIS, it will be available to the general public, including foreign nations.

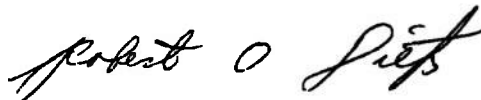
APPROVAL STATEMENT

This technical report has been reviewed and is approved for publication.

FOR THE COMMANDER



CARLOS TIRRES
Captain, USAF
Research and Development
Division
Directorate of Technology



ROBERT O. DIETZ
Director of Technology

UNCLASSIFIED

REPORT DOCUMENTATION PAGE		READ INSTRUCTIONS BEFORE COMPLETING FORM
1 REPORT NUMBER AEDC-TR-74-121	2 GOVT ACCESSION NO.	3 RECIPIENT'S CATALOG NUMBER
4 TITLE (and Subtitle) STATISTICAL PREDICTION OF MAXIMUM TIME-VARIANT INLET DISTORTION LEVELS		5 TYPE OF REPORT & PERIOD COVERED Final Report-July 1, 1972-June 30, 1974
		6. PERFORMING ORG. REPORT NUMBER
7 AUTHOR(s) J. L. Jacocks and K. R. Kneile, ARO, Inc.		8. CONTRACT OR GRANT NUMBER(s)
9 PERFORMING ORGANIZATION NAME AND ADDRESS Arnold Engineering Development Center Arnold Air Force Station, Tennessee 37389		10. PROGRAM ELEMENT, PROJECT, TASK AREA & WORK UNIT NUMBERS Program Element 65802F
11 CONTROLLING OFFICE NAME AND ADDRESS Arnold Engineering Development Center (DYFS) Arnold Air Force Station, Tennessee 37389		12 REPORT DATE January 1975
		13 NUMBER OF PAGES 74
14 MONITORING AGENCY NAME & ADDRESS (if different from Controlling Office)		15. SECURITY CLASS. (of this report) UNCLASSIFIED
		15a DECLASSIFICATION/DOWNGRADING SCHEDULE N/A
16 DISTRIBUTION STATEMENT (of this Report) Approved for public release; distribution unlimited.		
17 DISTRIBUTION STATEMENT (of the abstract entered in Block 20, if different from Report)		
18 SUPPLEMENTARY NOTES Available in DDC		
19 KEY WORDS (Continue on reverse side if necessary and identify by block number) mathematical prediction inlet levels time statistical analysis bandwidth time-varying value (extreme) distortion acquisition		
20 ABSTRACT (Continue on reverse side if necessary and identify by block number) Time-variant inlet pressure data from several aircraft designs are analyzed utilizing tools based on Gumbel's extreme-value statistics with the results illustrating the basic randomness of distortion factors. A probabilistic model of distortion is proposed with three parameters to be evaluated by fitting to inlet data by the method of maximum likelihood. The effects of data acquisition time, frequency bandwidth, and		

UNCLASSIFIED

UNCLASSIFIED

20. ABSTRACT (Continued)

sampling rate are discussed in context with Moore's similarity parameter to indicate scalability of the dynamic inlet distortion data. The end result of these analyses is a recommended procedure that enables the use of a short time segment of distortion data to statistically predict the expected maximum distortion level corresponding to any time period of inlet operation.

PREFACE

The work reported herein was sponsored by the Arnold Engineering Development Center (AEDC), Air Force Systems Command (AFSC), under Program Element 65802F. The research results presented were obtained by ARO, Inc. (a subsidiary of Sverdrup & Parcel and Associates, Inc.), contract operator of the AEDC, AFSC, Arnold Air Force Station, Tennessee. The research was conducted from July 1, 1972 through June 30, 1974, under ARO Project Nos. PF212 and PF412 with Captain C. Tirres as Project Monitor. The manuscript (ARO Control No. ARO-PWT-TR-74-81) was submitted for publication on September 16, 1974.

CONTENTS

	<u>Page</u>
1.0 INTRODUCTION	5
2.0 BACKGROUND	
2.1 General Discussion	6
2.2 Randomness of Engine-Face Pressure Patterns	6
2.3 Randomness of Distortion Factors	10
3.0 PRINCIPLES OF EXTREME-VALUE STATISTICS	
3.1 Asymptotic Theory of Extremes	10
3.2 Parameter Estimation	12
3.3 Return Period	14
3.4 Variance Estimates	16
4.0 APPLICATIONS TO INLET DISTORTION DATA	
4.1 Effect of Number of Extremes	19
4.2 Effect of Frequency Bandwidth	29
5.0 RECOMMENDED PROCEDURES FOR ANALYSIS OF INLET DISTORTION	
5.1 Inlet Development Testing	34
5.2 Inlet/Engine Compatibility Demonstration	35
5.3 Data Processing	36
6.0 CONCLUDING REMARKS	38
REFERENCES	38

ILLUSTRATIONS

Figure

1. Representative Digital Instantaneous Distortion Results	7
2. Typical Engine-Face Total-Pressure Waveforms at the Time of Peak Distortion	9
3. Comparison of the First and Third Asymptotes with Inlet Distortion Data	13
4. Interpretation of Extreme-Value Statistics Utilizing the Reduced Variate and Return Period Concepts	15
5. Tolerance Band Dependence on Data Quantity	18
6. Representative Comparisons of Predicted and Observed Peak Instantaneous Distortion	20
7. Dependence of the Expected Extreme on the Number of Independent Samples for the Chi-Square Distribution Family	28
8. Dependence of the Modal Value on the Number of Extremes	29

<u>Figure</u>	<u>Page</u>
9. Effect of Frequency Bandwidth on Peak Distortion Magnitude	30
10. Computed Probability Density Distributions with Variation of Moore's Similarity Parameter	31
11. Effect of Frequency Bandwidth on the Normalized Modal Distortion	32
12. Effect of Frequency Bandwidth on the Number of Zero Crossings	32
13. Dependence of the Normalized Modal Distortion on the Ratio of Zero Crossings to Number of Extremes	34

APPENDIXES

A. DISTORTION FACTOR FORMULATIONS	41
B. ANALYTIC DETAILS	47
C. COMPUTER PROGRAM DETAILS	54
NOMENCLATURE	73

1.0 INTRODUCTION

Most aircraft engine manufacturers have developed empirical distortion factors which correlate engine stability degradation with the spatial variation of inlet recovery. Over the years these factors have evolved from simple parameters based on steady-state pressures to complicated formulations using instantaneous values of high-frequency bandwidth dynamic pressures with sampling rates comparable to the engine rotation frequency. The time-variant nature of inlet distortion has led to the use of a new descriptor, peak instantaneous distortion (which is the maximum magnitude of any particular distortion factor observed at a given test condition), and it is perhaps the major parameter for the definition of inlet/engine compatibility. Inlet development tests have also used the peak instantaneous distortion as a standard of comparison in various optimization cycles, selecting the geometry or bleed rate which yielded the lower distortion without compromising other performance criteria. However, as shown in Ref. 1, the peak instantaneous distortion is an inconsistent indicator of inlet performance since the observed magnitude is dependent on data acquisition time, and repeat test conditions can yield significantly different results even if data acquisition time were held constant. These facts are directly the result of distortion factors being random variables when calculated from stationary dynamic pressure measurements (stationary meaning, for the present application, that the average and root-mean-square are constant with respect to time). It is therefore necessary that probabilistic analysis tools be utilized to interpret inlet distortion data and thereby obtain a statistical prediction of the maximum distortion level for each test condition.

The statistical analysis of Ref. 1 was based on Gumbel's (Ref. 2) first asymptotic distribution of extremes which postulates an unlimited distortion magnitude. This intuitively unacceptable requirement can be avoided by using a generalization of Gumbel's third asymptote which postulates an unknown upper bound to the distortion magnitude. Data from several inlet tests indicate that the generalized asymptote provides a better probabilistic model of distortion peaks than the first asymptote.

This report presents examples of the application of Gumbel's asymptotic theory of extremes to data acquired in several inlet tests and illustrates the general statistical properties of various distortion factors. The distribution of extremes is characterized by a three-parameter Weibull distribution. The parameters are estimated by the method of maximum likelihood (Ref. 3, for example) using a modified Gauss-Newton iteration technique (Ref. 4). The effects of data acquisition time, frequency bandwidth, and sampling rate are discussed in context with Moore's similarity parameter, λ , (Ref. 5) to indicate scalability of the dynamic inlet distortion data. The end result of these analyses is a recommended procedure for the prediction of maximum time-variant inlet distortion levels with error tolerance estimates to the desired degree of confidence.

2.0 BACKGROUND

2.1 GENERAL DISCUSSION

Recent aircraft and engine development programs for high-performance vehicles have pushed the problem of inlet/engine compatibility to the forefront of designer's concern. Enlarged Mach number-altitude-attitude operating envelopes have resulted in a decrease in the uniformity and an increase in the turbulence of the flow delivered to the engine while engine operating lines have been raised to achieve maximum practicable thrust levels. Working stall margins are minimal, and the major degradation of the surge line is allotted to inlet distortion.

The inlet flow nonuniformity is usually expressed in terms of total-pressure distortion because of measurement ease. Typically, eight rakes of total-pressure probes with five to six probes per rake (see Fig. A-1) are used to measure the pressure profile of the inlet/engine interface plane of low-bypass turbofan installations. Experience with the B-70 and F-111 programs (Refs. 6 and 7) has demonstrated that engines are sensitive to time-variant inlet distortion with minimum response times comparable to the compressor rotation period. Measurements of the engine face pressures are thus required with relatively high-frequency bandwidths for full-scale testing and wider bandwidths (inversely proportional to scale) for the sub-scale inlet development tests. Informal industry standards have evolved for the measurement and acquisition of these data, the miniature transducers being housed in probes of the Hoeflinger-type (Ref. 8) and the data being recorded on 14-track analog tapes in multiplexed constant-bandwidth FM mode. Data acquisition times are typically equivalent to 2 to 3 minutes of full-scale inlet/engine operation for stationary test conditions.

Real-time analog processors have been developed (Refs. 5 and 9) to calculate the various distortion factors (see Appendix A), screen the data, and locate the instant of time at which the maximum distortion occurred. If the test condition is considered sufficiently important, a short time segment of data containing the observed analog peak distortion is then digitally processed to achieve greater accuracy than available from the real-time processor and to obtain the engine-face pressure profile at the instant the peak distortion occurred.

2.2 RANDOMNESS OF ENGINE-FACE PRESSURE PATTERNS

An example of a typical distortion index which has been calculated from the digitized, time-varying engine-face total pressures for a two-dimensional inlet system is shown in Fig. 1. Constant-pressure contour maps are also given for the time-averaged (steady-state) data and for the instant of peak distortion wherein the lines represent the difference

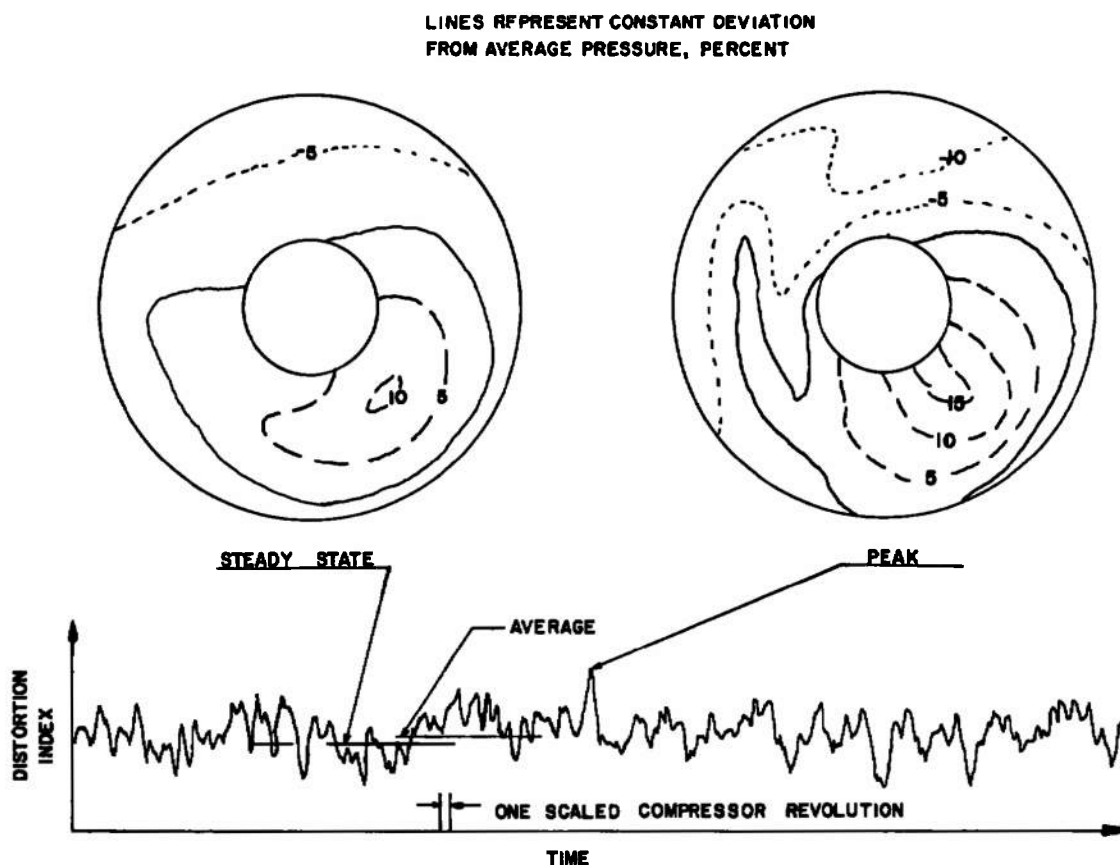


Figure 1. Representative digital instantaneous distortion results.

between the local total pressure and the face average, normalized by the engine-face average pressure. The time-variant distortion fluctuates randomly about an average distortion level that is comparable to (but greater than*) the distortion calculated from steady-state instrumentation. At some instant, the relative maximum distortion for this time interval is noted, termed peak instantaneous distortion, and the associated engine-face pressure pattern may or may not be similar in shape to the steady-state pattern. For a low-turbulence inlet operating condition the pattern at the instantaneous peak distortion time is quite similar to the steady-state pattern shape, differing only in intensity level. Medium turbulence levels generally result in peak distortion patterns which vaguely resemble the steady-state shape, whereas for high-turbulence conditions, the pressure patterns at instants of peak distortion are quite dissimilar and agreement in shape with the steady-state pattern is a rare occurrence.

*As a result of nonlinearities in all distortion factor formulations used for this report and the types of turbulence encountered, the mean level of distortion was always equal to or greater than the level computed from the mean pressures. As an example, imagine a turbulent flow field superimposed on a uniform (zero distortion) steady-state pressure pattern, for this case the average time-variant distortion level would be positive and increase with increasing turbulence levels.

A visual appreciation for the randomness of the total-pressure fluctuations may be gained from Fig. 2. This figure shows the end result of screening a long-time segment (minutes) of inlet operation via an analog computer, subsequently digitizing the recorded pressure data in the vicinity of the time of peak instantaneous distortion as indicated by the analog processor, and then digitally calculating the distortion as a function of time. For comparison, the steady-state and peak instantaneous distortion pressure patterns are shown, as well as the time histories of each individual measured total pressure referenced to the local steady-state pressure. The normalized pressure wave forms about the time of peak distortion show little spatial correlation and it is clear from this and other analyses that increasing turbulence levels would cause greater dissimilarity between the peak pattern and the steady-state pattern. Moreover, the basic randomness of the time-dependent flow results in the pressure pattern at the time of the instantaneous peak distortion being one sample from an uncountable population of patterns, hence the engine-face pressure pattern corresponding with the peak instantaneous distortion is not repeatable. The peak distortion pattern given in Fig. 2 may eventually be generated by that inlet again, but the only reproducible data in Fig. 2 are the steady-state pressures or other time-averaged quantities.

The distortion factor methodology as developed by engine manufacturers is the result of correlating engine sensitivity to varied screen-generated pressure patterns with the objective of expressing engine surge margin as a function of distortion magnitude independently of pattern shape. Thus, inlet development testing can and should rely on the distortion factor methodology for assurance of inlet/engine compatibility without regard or concern about nonrepeatability of the instantaneous engine-face pressure patterns. However, the present report questions the current practice of engine qualification testing behind expensive screen simulation of the instantaneous pressure patterns obtained from sub-scale inlet model tests when the inlet may never generate that exact pattern again. Since qualification tests of engines subjected to representative extreme distortion patterns do provide necessary confidence with respect to inlet/engine compatibility, it is recommended that screens be designed with an approximate intensification of the steady-state distortion pattern. This could be a simple linear stretching of the pattern to a representative instantaneous distortion level or the "worst case projection" method of Kimzey and McIlveen (Ref. 10). The latter procedure should be more representative since the turbulence distribution and phase relationships between pressure fluctuations are an integral part of the method. Any desired distortion level can be achieved by selection of the "crest factors" (ratio of peak-to-peak over rms level of individual pressures) so that assurance of inlet/engine compatibility via screen testing could be achieved at any desired level of confidence. The particular distortion level to be selected is the subject of this report.

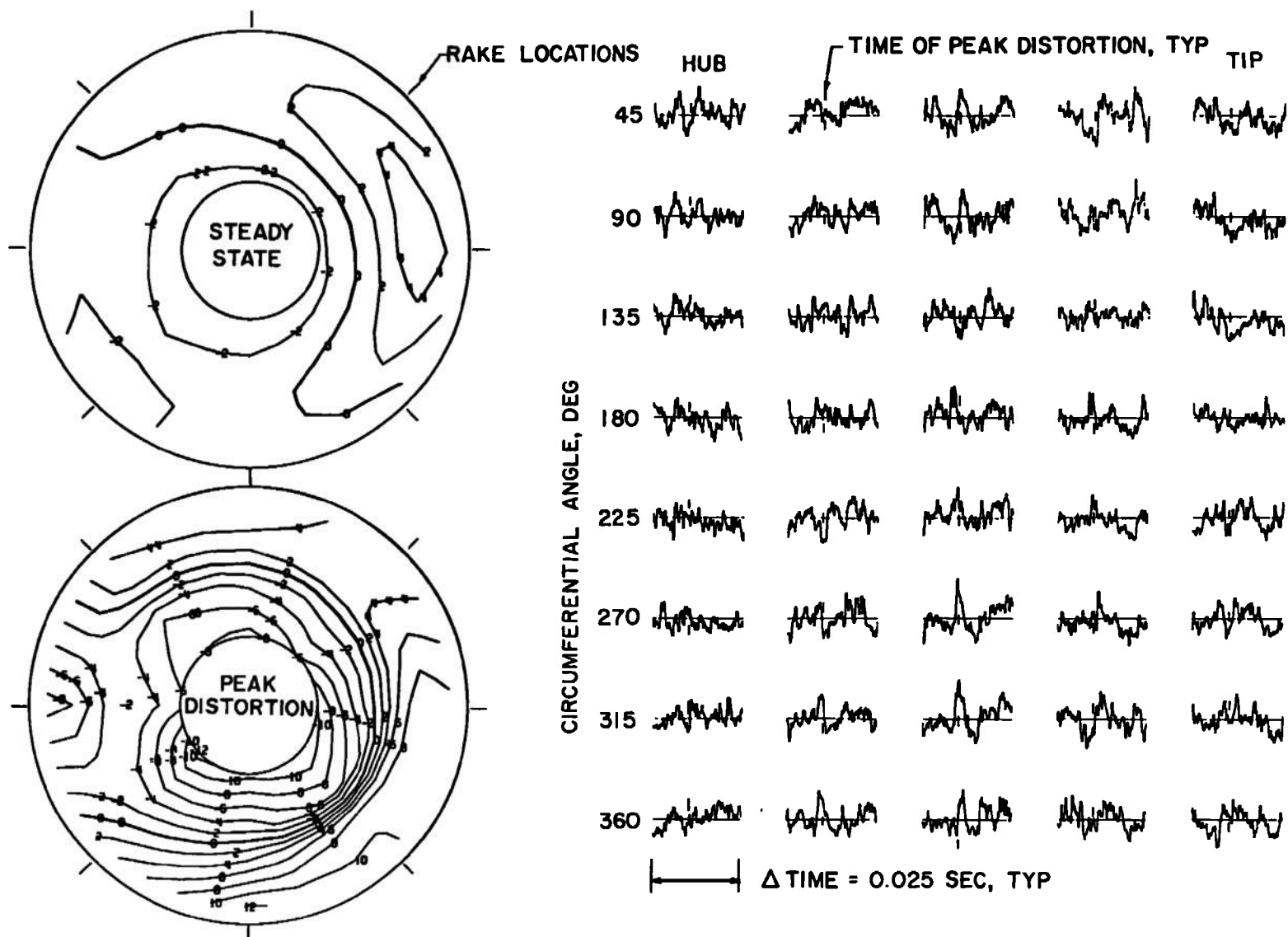


Figure 2. Typical engine-face total-pressure waveforms at the time of peak distortion.

2.3 RANDOMNESS OF DISTORTION FACTORS

Since the total-pressure fluctuations appear to be of a random nature and the various distortion factors are functions of those pressures, it follows that every distortion factor considered as a time sequence is representative of a stochastic process. Any instantaneous sample from that process is only one possible sample from an infinite population. In particular, the one observed peak instantaneous distortion within a finite observation or data acquisition time period is just that - one observation. Admittedly, if an engine stalls as a result of the distortion level, then that one observation assumes special significance. The major objective of this report is to offer a means for interpreting time-variant inlet distortion data obtained during inlet development tests, a period when no engine is present to do the job of interpreting distortion levels.

The first step will be to estimate the probability distribution of a distortion factor. It is assumed that the inlet flow process is stationary, that is, the statistical properties of the distortion factor are invariant with time. It is further assumed that the process is ergodic so that these statistical properties may be estimated from a single time sequence and may be used to describe future realizations. For determination of inlet/engine compatibility one is interested in the maximum distortion levels, not with average levels, so that conventional methods of describing the distribution using central moments would not be appropriate. Gumbel's statistical theory of extreme values (Ref. 2) is used because in addition to the obvious suitability for analysis of maxima, it also eliminates the need to select a restrictive family of distributions a priori.

3.0 PRINCIPLES OF EXTREME-VALUE STATISTICS

3.1 ASYMPTOTIC THEORY OF EXTREMES

The theory of extremes is a study of the statistical properties of observations that are extreme in comparison to other values observed from the same population. An example, and Gumbel's prototype, is the water flow of a river where floods are considered as extreme. Gumbel's theory of extremes provides the analysis tool for estimating the sizes of future floods. For the present study, the maximum observed distortion during a period of time is considered as an extreme value.

The starting point* for the theory of extremes is the distributional properties of the maximum of n independent observations from the same population. Let X_1, X_2, \dots ,

*Gumbel's remark seems appropriate - "the exact distributions of extreme values are easy to obtain and well known. Yet every new worker in the vast field of breaking strength appears to find it necessary to derive them over and over again."

X_n denote n observations from the same parent population and let X be the maximum of X_i . The cumulative probability function of X is then given by

$$\begin{aligned}
 F(x) &= \text{Prob} (X \leq x) \\
 &= \text{Prob} (\text{all } X_i \leq x) \\
 &= \prod_{i=1}^n \text{Prob} (X_i \leq x) \\
 &= \Phi^n (x)
 \end{aligned} \tag{1}$$

Thus, the distribution $F(x)$ of the maximum of n observations is easily related to the distribution $\Phi(x)$ of the parent population. The practicality of this expression is limited to cases where the original distribution is known. The major contribution from the theory of extremes is that, for large n , the distribution $F(x)$ has a known asymptotic form. Gumbel (Ref. 2) gives three asymptotic forms depending upon assumptions about the nature of the parent or initial distribution $\Phi(x)$.

Gumbel's first asymptote postulates an initial distribution which is unlimited to the right with all moments existing (e.g. normal, exponential) and can be written with two parameters, a_1 , as

$$F_1(x) = \exp [- \exp [-a_1(x-a_2)]] \tag{2}$$

Gumbel's second asymptote postulates an initial distribution which is also unlimited to the right but with some or all moments undefined because of a large right tail (e.g. Cauchy) and can be written with two parameters, b_1 , as

$$F_2(x) = \exp [- (b_1/x)^{b_2}] \tag{3}$$

Gumbel's third asymptote postulates an initial distribution which is limited to the right (e.g. Weibull reversed) and can be written with three parameters, c_1 , as

$$F_3(x) = \exp - \left[\frac{c_1 - x}{c_1 - c_2} \right]^{c_3} \tag{4}$$

As given in Appendix B, all three asymptotes can be restated in a single generalized asymptotic distribution of extremes in the form

$$F(x) = \exp - \left[\frac{a - \beta x}{a - \beta v} \right]^{1/\beta} \tag{5}$$

In terms of application to distortion data, the ratio a/β is the maximum level achievable, the parameter ν may be thought of as the most frequently occurring extreme distortion level (mode), the parameter a represents approximately the rate of increase of distortion with the logarithm of time, and β is the distinguishing parameter for the three asymptotes ($\beta = 0$ corresponds to the first asymptote, $\beta < 0$ is the second asymptote, and $\beta > 0$ is the third asymptote.)

Defining a reduced variate t as (where \log represents natural logarithm),

$$t \equiv -\log \log 1/F(x) \quad (6)$$

the inverse of Eq. (5) can be written as

$$x = \frac{a}{\beta} - \left[\frac{a}{\beta} - \nu \right] e^{-\beta t} \quad (7)$$

and the inverse of the first asymptote is the linear expression

$$x = a_2 + t/a_1 \quad (8)$$

where, for $\beta = 0$, the generalized asymptote reduces to $a = 1/a_1$ and $\nu = a_2$.

Although Ref. 1 recommended utilization of the first asymptote, further distortion data analyses in the form of Fig. 3 have shown the extremes of time-variant inlet distortion to be better described by the generalized asymptote. (Discussion of the procedure for generating the information contained in Fig. 3 is delayed until Section 5.3.) In this typical example, the distortion data clearly deviate from the first asymptote or straight line ($\beta = 0$) and, for specific values of the parameters a , β , and ν the generalized (third) asymptote provides a good fit to the data. Given that the general asymptote is a good representation of the cumulative probability distribution of distortion extremes, there remains the problem of determining the parameters a , β , and ν .

3.2 PARAMETER ESTIMATION

The general asymptote describes a broad family of distributions dependent on the parameters a , β , and ν which in turn are an unknown function of the inlet flow processes and distortion factor formulation. This lack of knowledge is circumvented herein by postulating that one has observed N distortion extremes X_i , each selected from a fixed time interval Δt , covering a total time period $N\Delta t$ of inlet operation. (Note that the time intervals are not necessarily contiguous.)

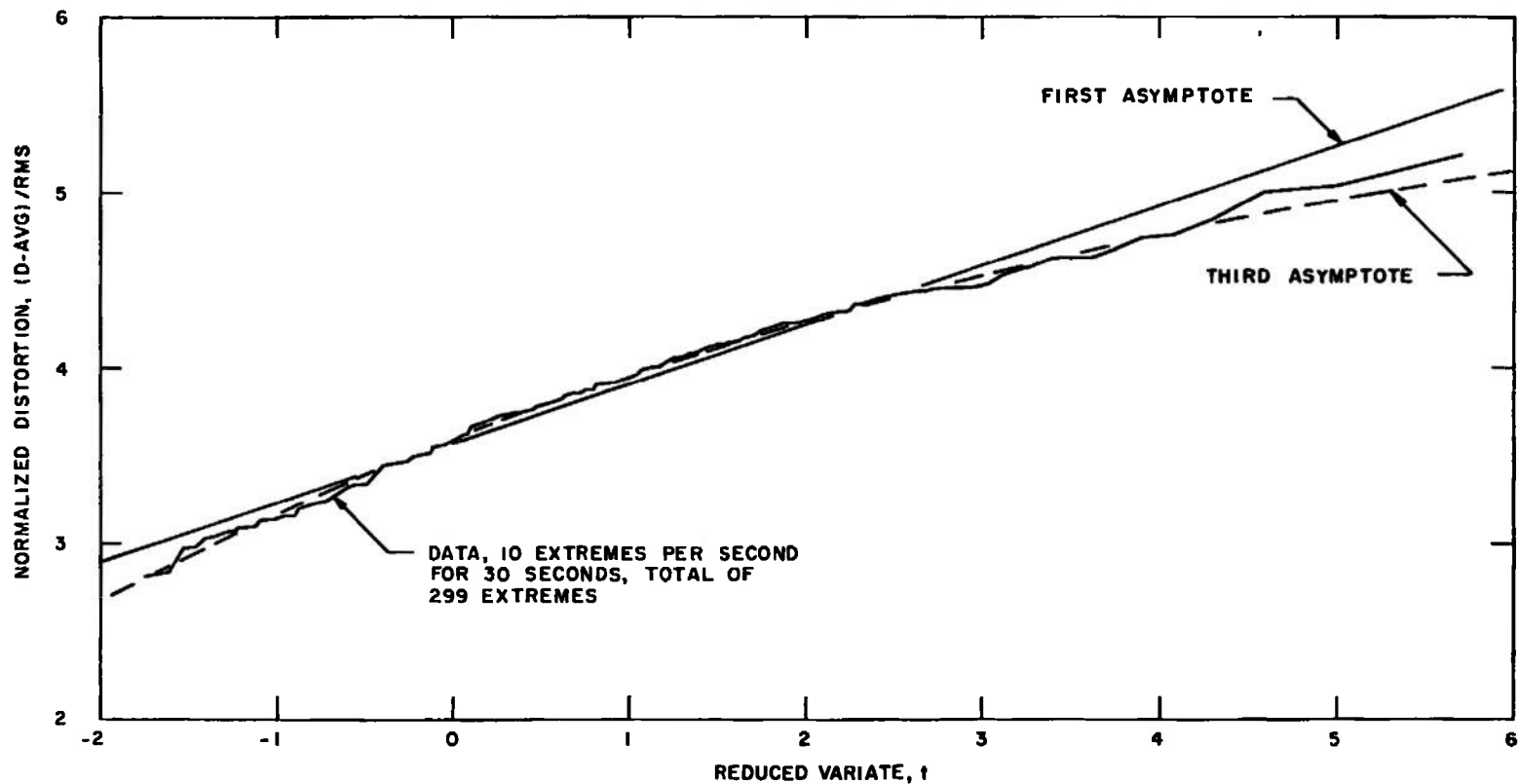


Figure 3. Comparison of the first and third asymptotes with inlet distortion data.

Gumbel presents several methods for estimating the parameters and, although these methods were relatively simple to use, the resulting estimates were not satisfactory*. The authors also attempted parameter estimation with a nonlinear least squares fit to the cumulative distribution of the order statistic, the latter being given by

$$F(x) = i/(N+1) \quad (9)$$

where the X_i are arranged in ascending order ($X_1 \leq X_2 \leq \dots \leq X_N$). The difficulties with this method arise from the fact that the elements of the order statistic are not independent. While ignoring this fact may still give reasonable parameter estimates, the interdependence must be used in determining the variance of the estimate. Even though this method was rejected, the cumulative distribution of the order statistic was retained as a visual aid for comparison with the distribution estimated parametrically. That is, the observed data are plotted (as in Fig. 3) using the ordered X_i versus t_i where

$$t_i = -\log \log \frac{N+1}{i}$$

The method of parameter estimation accepted by the authors used the principle of maximum likelihood. This method gave the best results, avoided the a priori selection of the asymptotic type, and yielded reasonable variance estimates. Details of the procedure are given in Appendix B.

3.3 RETURN PERIOD

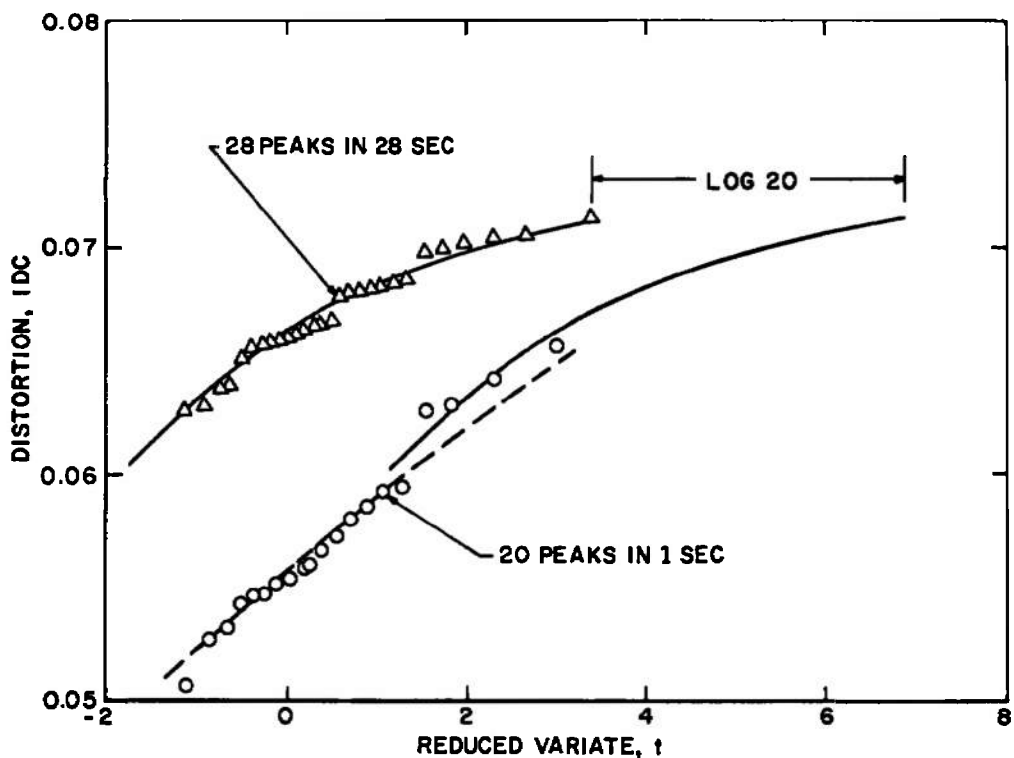
Gumbel has developed a return period concept which enables interpretation of the probability levels (or magnitudes of the reduced variate) in terms of natural units of time, which makes comprehension somewhat easier. In functional form the return period is defined by

$$T = \frac{1}{1-F(x)} = \frac{1}{1-\exp(-\exp(-t))} \quad (10)$$

and represents the median number of observations necessary to obtain one value equal to or larger than x . Since the distortion extremes are selected from a specific time interval Δt , the number of observations T is also the number of time intervals, hence the return period represents the inlet operation time required to observe (on the average) one distortion extreme greater than x .

*Simulated results showed large variances for the estimates, formulas for variances were not available for all methods, and in most cases the type of asymptote had to be selected a priori.

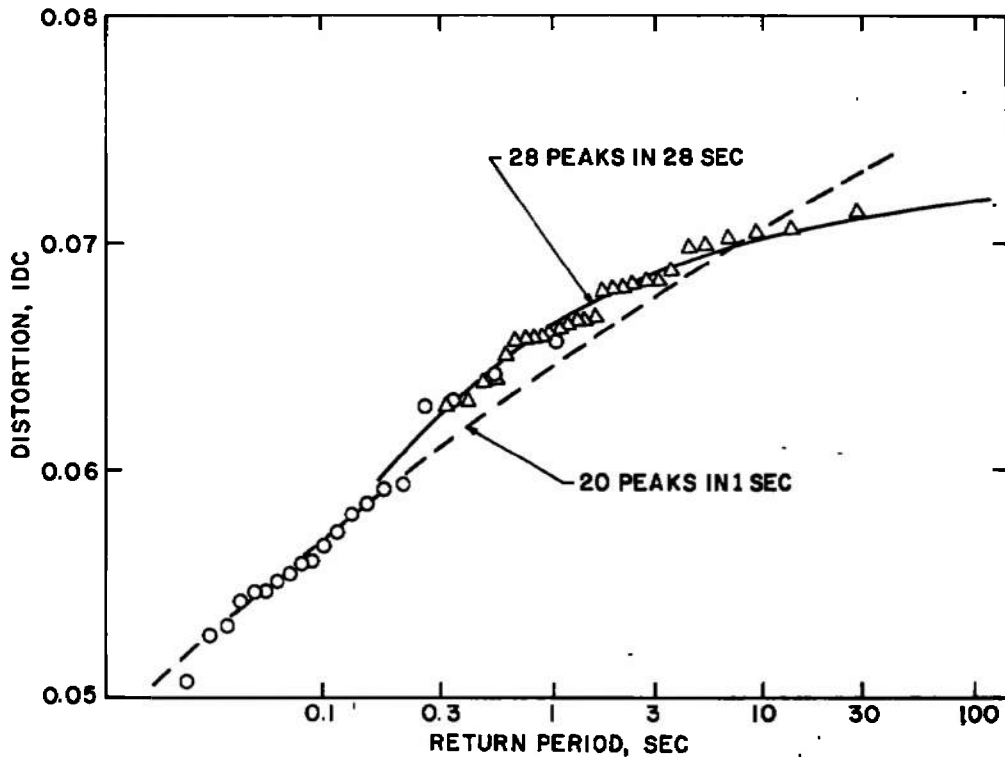
If analysis of distortion data is attempted using two sets of observations from the same test condition with differing time intervals, then seemingly disparate results may be obtained as illustrated by Fig. 4a. The difficulty is that one of the parameters of the asymptotic distribution is a function of the time interval because the expected distortion level increases approximately* as the logarithm of time. As developed in Appendix B, consistent results can be obtained by redefining the reduced variate t for one set of data so that the curve is shifted laterally by the logarithm of the time interval ratio. For the example given in Fig. 4a, each extreme within the 28-point set was selected from a time interval twenty times longer than the extremes of the 20-point set, thus the shift should be $\log 20$, and indeed this does yield consistent results. An alternate presentation (Fig. 4b), the recommended one, can be made using the return period (with physical units of time) which bypasses the necessity of maintaining a fixed time interval among multiple data sets.



a. Reduced variate concept

Figure 4. Interpretation of extreme-value statistics utilizing the reduced variate and return period concepts.

*Exactly for the first asymptote.



b. Return period concept
Figure 4. Concluded.

The results given in Fig. 4 also illustrate the power of extreme value statistics: one second of inlet distortion measurements can yield answers comparable to the results of a much longer time period of inlet operation. A short time segment of distortion data can be used to statistically predict future distortion levels.

3.4 VARIANCE ESTIMATES

One of the advantages of using the method of maximum likelihood for estimation of the three parameters of Eq. (5) was the ability to also estimate the variance (or accuracy) of the result. As detailed in Appendix B, the intermediate results used in computation of the parameter estimates can be used to form the variance-covariance matrix of the three parameters. Expansion of Eq. (7) by a Taylor series about any desired probability level then allows estimation of the variance of the distortion corresponding to that probability level. Since the probability level can be related to the return period, one can therefore estimate the variance of the expected peak distortion corresponding to any time period of inlet operation.

Since the parameters are asymptotic normally distributed, one-sigma tolerance bands constructed from these variances represent nominally 68-percent confidence levels. However, comparisons of the statistical prediction of a future distortion level with an observed peak distortion data point require consideration of variance of this future observation. That is, the peak instantaneous distortion within a finite data acquisition time period is itself a random variable so that comparisons between the observed and predicted level must allow for variances from both sources. As detailed in Appendix B, the variance of the peak instantaneous distortion decreases with increasing data acquisition time (provided $\beta > 0$) so that for large times the observational variance is usually negligible relative to the parameter estimation variance.

The one-sigma tolerance bands are of course dependent on the data and generally become smaller with increasing number of extremes. As an example, the effect of using 5 extremes per second for the initial six and twelve seconds out of a two-minute record is illustrated by Fig. 5. The tolerance bands of Fig. 5b are clearly more narrow than those of Fig. 5a and, generally speaking, the bands decrease in proportion to \sqrt{N} (N being the number of extremes) as they should for normally distributed parameters. The solid symbol in Fig. 5 is the peak instantaneous distortion for the full two minutes. Note that the one-sigma tolerance bands become larger with increasing return period and are smallest in the vicinity of $t = 0$.

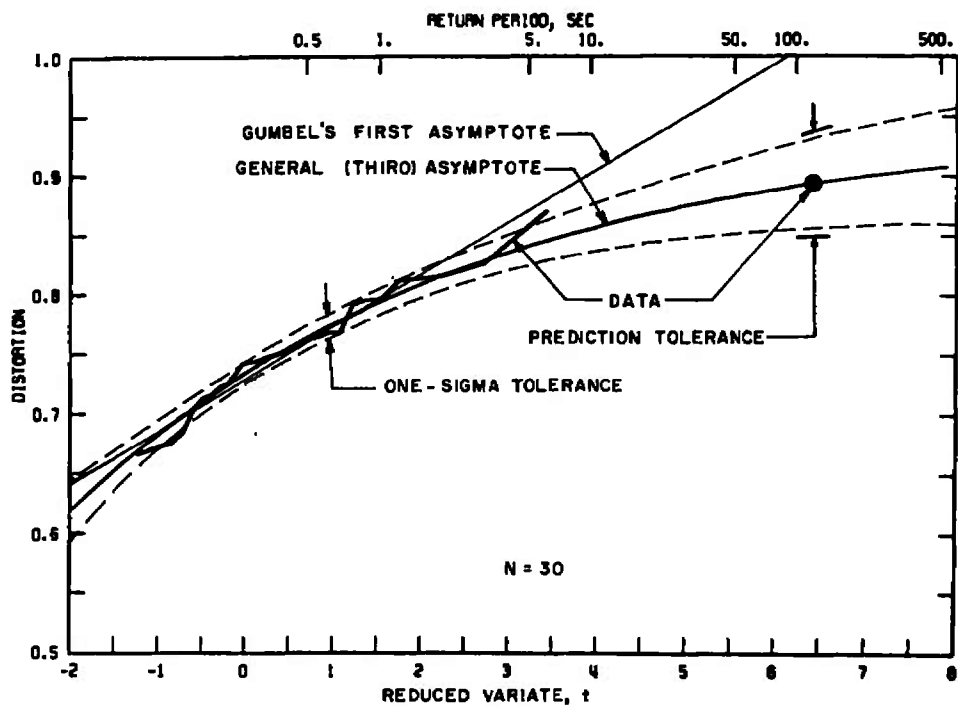
The mode or most probable distortion level is given by

$$y_m = a/\beta - (a/\beta - \nu)(1 - \beta)^{\beta} \quad (11)$$

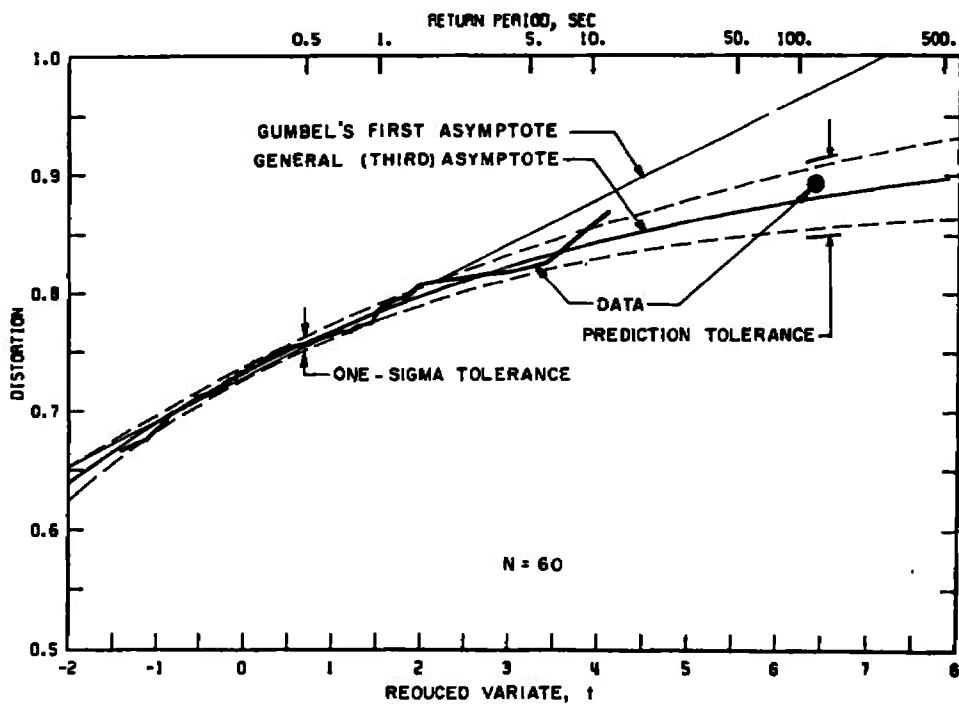
and in the limit of $\beta \rightarrow 0$, $y_m = \nu$, which is the distortion magnitude at $t = 0$. Since most distortion data result in small β as will be shown and the estimation tolerance is near minimum at $t = 0$, the parameter ν is termed the modal value and will be used herein as the major descriptor of peak distortion levels.

The estimation tolerance is generally quite large for the limiting distortion level $\epsilon = a/\beta$ when estimated from a practicable number of extremes. Typical tolerance results for ϵ are ± 100 percent when computed from 60 extremes selected from twelve seconds of distortion data akin to Fig. 5b, whereas tolerances on the order of ± 5 percent may be expected from data like that of Fig. 3*. Therefore, one should generally not attempt extrapolation of the extreme-value results beyond more than, say, 100 times the basic observational time unless the tolerances indicate otherwise.

*Due to inlet scale, Fig. 3 effectively represents approximately twelve times the total data quantity of Fig. 5b.



a. Thirty extremes



b. Sixty extremes

Figure 5. Tolerance band dependence on data quantity.

To provide insight and an appreciation for the overall accuracy of the analysis, several examples are presented in Fig. 6, each case being twelve seconds of data with the extrapolation compared to a two-minute peak instantaneous distortion point similar to that given in Fig. 5b. These examples cover a wide range of Mach number, inlet geometry, and airflow and are typical of data acquired at AEDC with a variety of inlet designs. (The reader is cautioned not to infer an approximate constant slope, in that each example generally uses a different ordinate scale.) The line codes of Fig. 6 are the same as used in Fig. 5. The primary conclusion gained from these examples is that the tolerance bands are applicable to prediction of future distortion levels.

4.0 APPLICATIONS TO INLET DISTORTION DATA

In the preceding sections the development of extreme-value statistics and its relation to time-variant inlet distortion were discussed. Some practical aspects that should be considered when using the techniques for routine analysis of inlet distortion data are given in the following sections.

4.1 EFFECT OF NUMBER OF EXTREMES

Application of extreme-value statistics to time-variant inlet distortion data requires the arbitrary selection of two time intervals: the total data time length t for which analysis is desired and the incremental time Δt from which each extreme will be chosen. The number of extremes N is the ratio $t/\Delta t$. As developed in Appendix B, the parameters α and β are independent of Δt , whereas the modal value ν is a function of Δt .

As an illustration of the effect of the incremental time Δt , Eq. (1) has been used with tabulations (Ref. 11) of the Chi-square family of probability functions to compute the expected level of an extreme as a function of n , the number of independent samples. For demonstration purposes, assume the time interval Δt to be proportional to the effective number of independent observations. The results are given as Fig. 7 with the mode considered as a standardized variable. The asymptotic form of the Chi-square family is Gumbel's first asymptote, thus Fig. 7 also provides some insight as to the number of independent observations required to allow its use with an a priori selected parent population. For example, if one knew the parent population had a Chi-square distribution with only a few degrees of freedom, then extremes selected from small samples could accurately be analyzed with the first asymptote, whereas large degrees of freedom require much larger samples for the first asymptote to be valid. That is, the first asymptote is applicable if the expected extreme is a linear function of the logarithm of the number of independent samples.

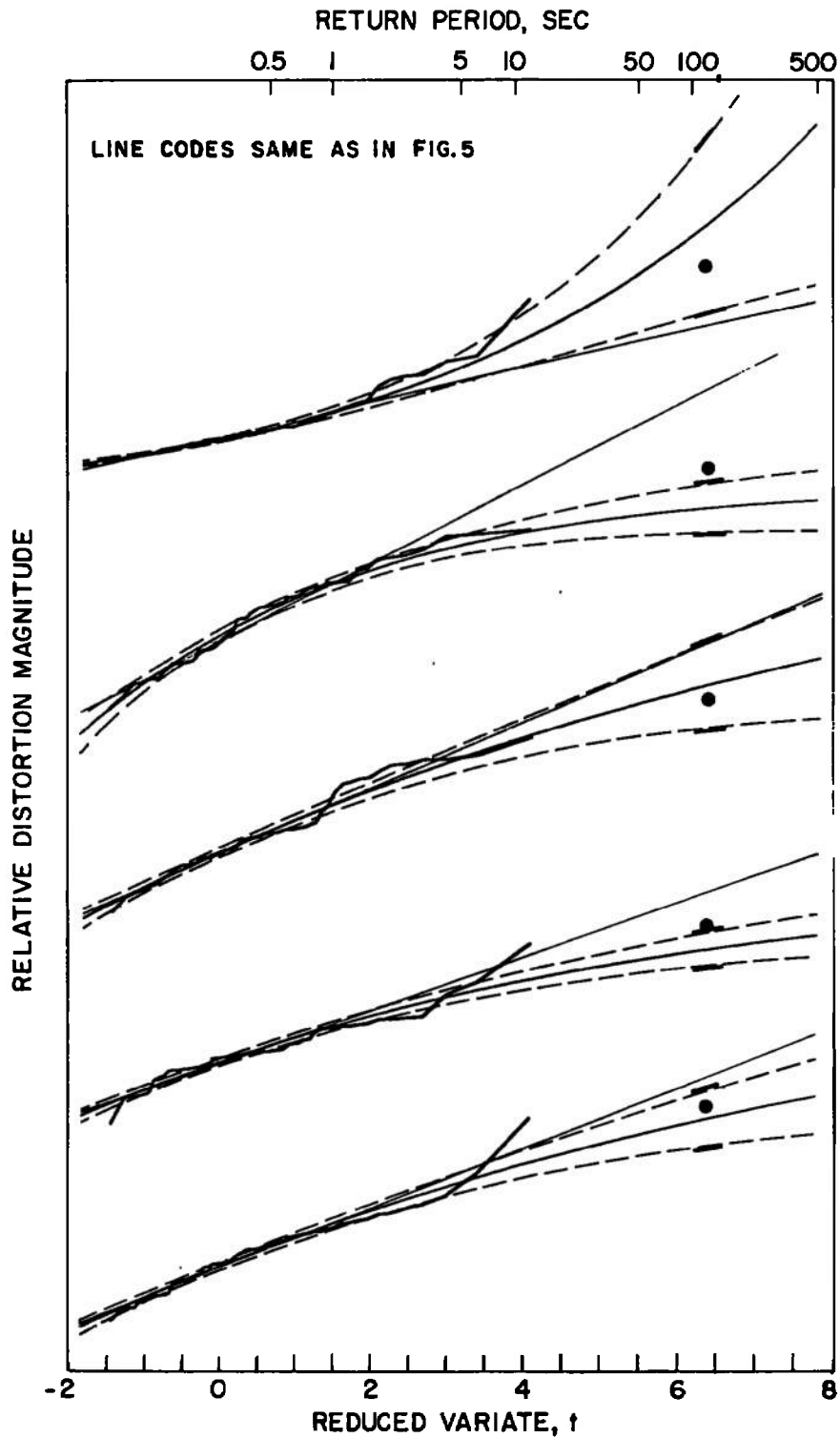


Figure 6. Representative comparisons of predicted and observed peak instantaneous distortion.

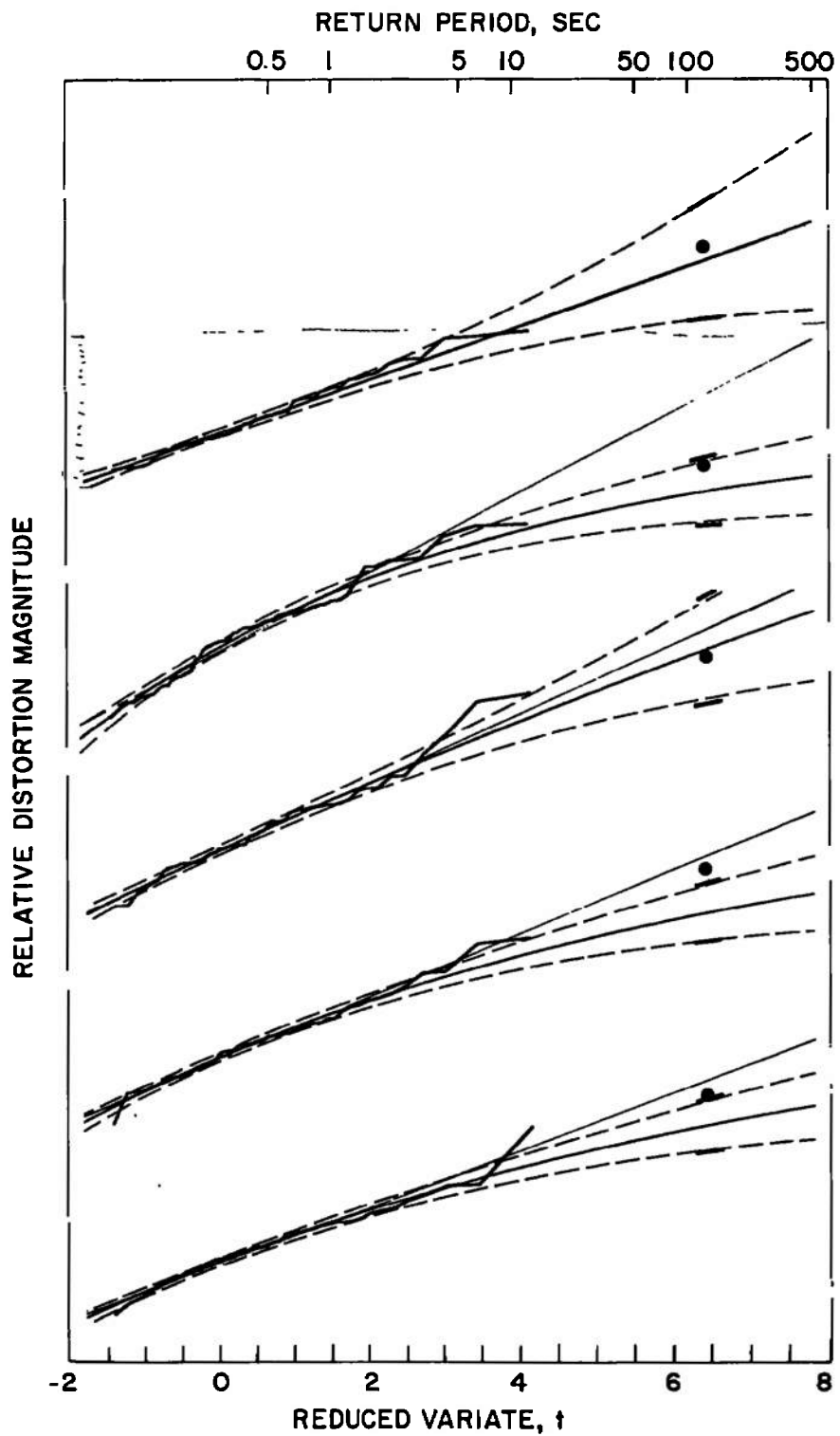


Figure 6. Continued.

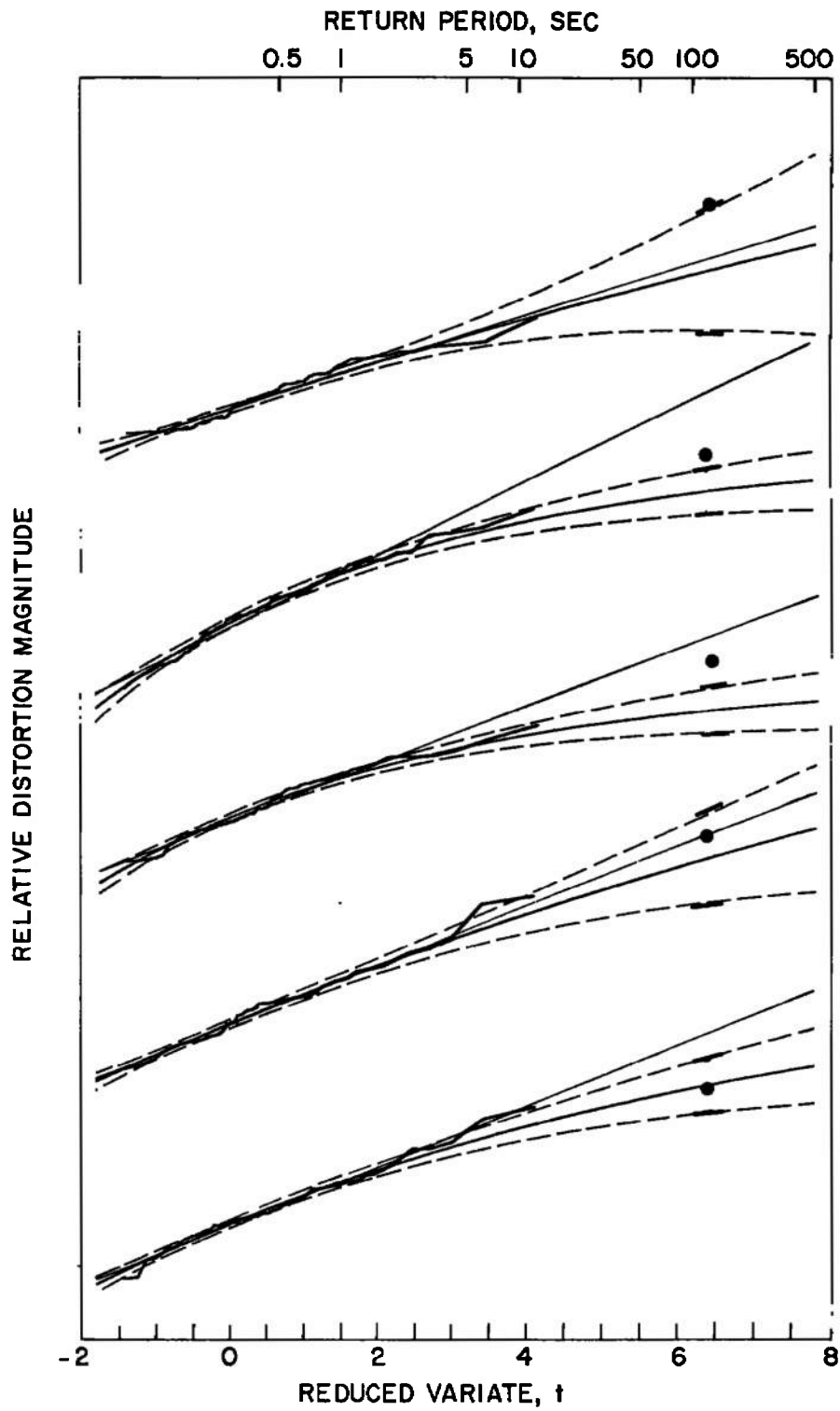


Figure 6. Continued.

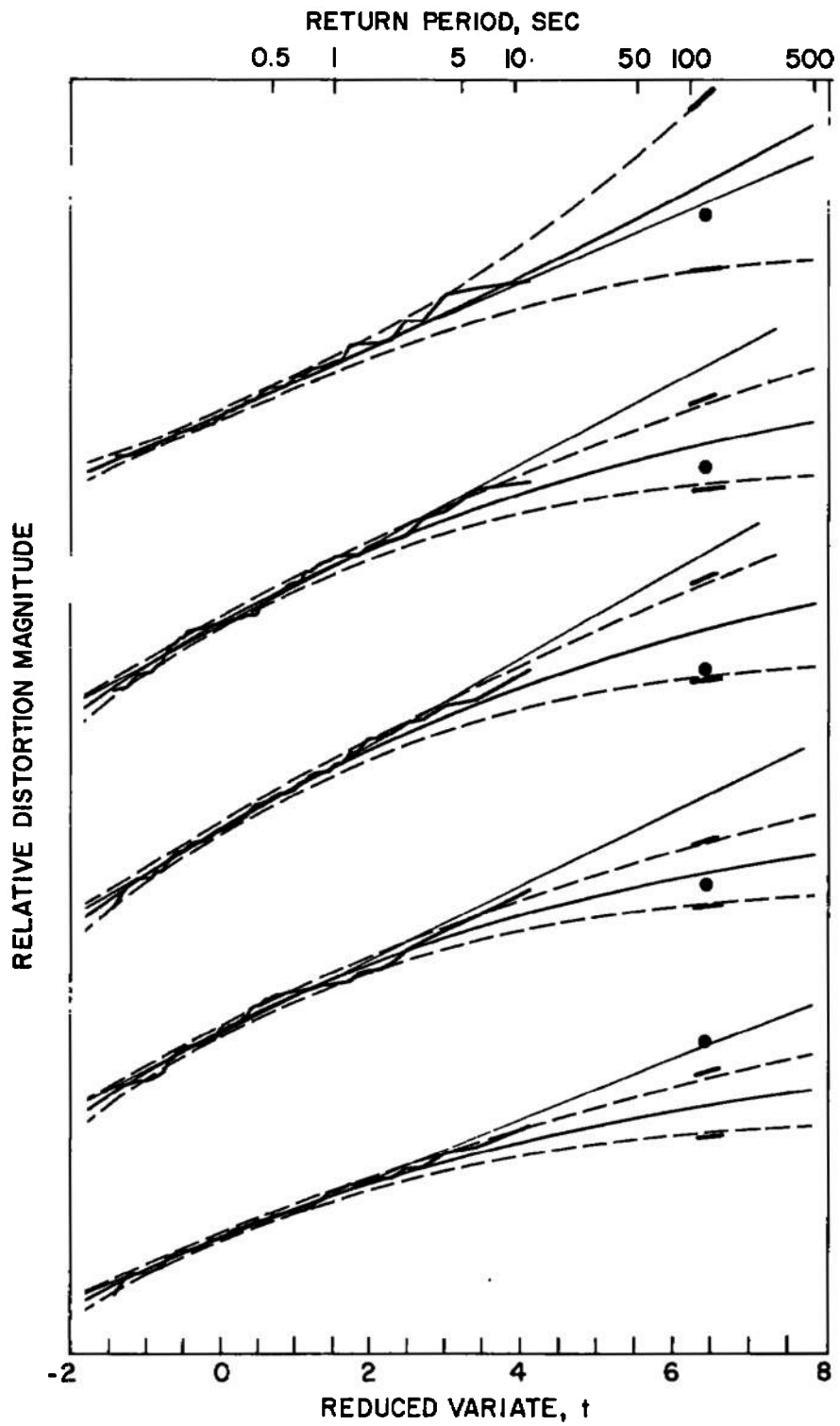


Figure 6. Continued.

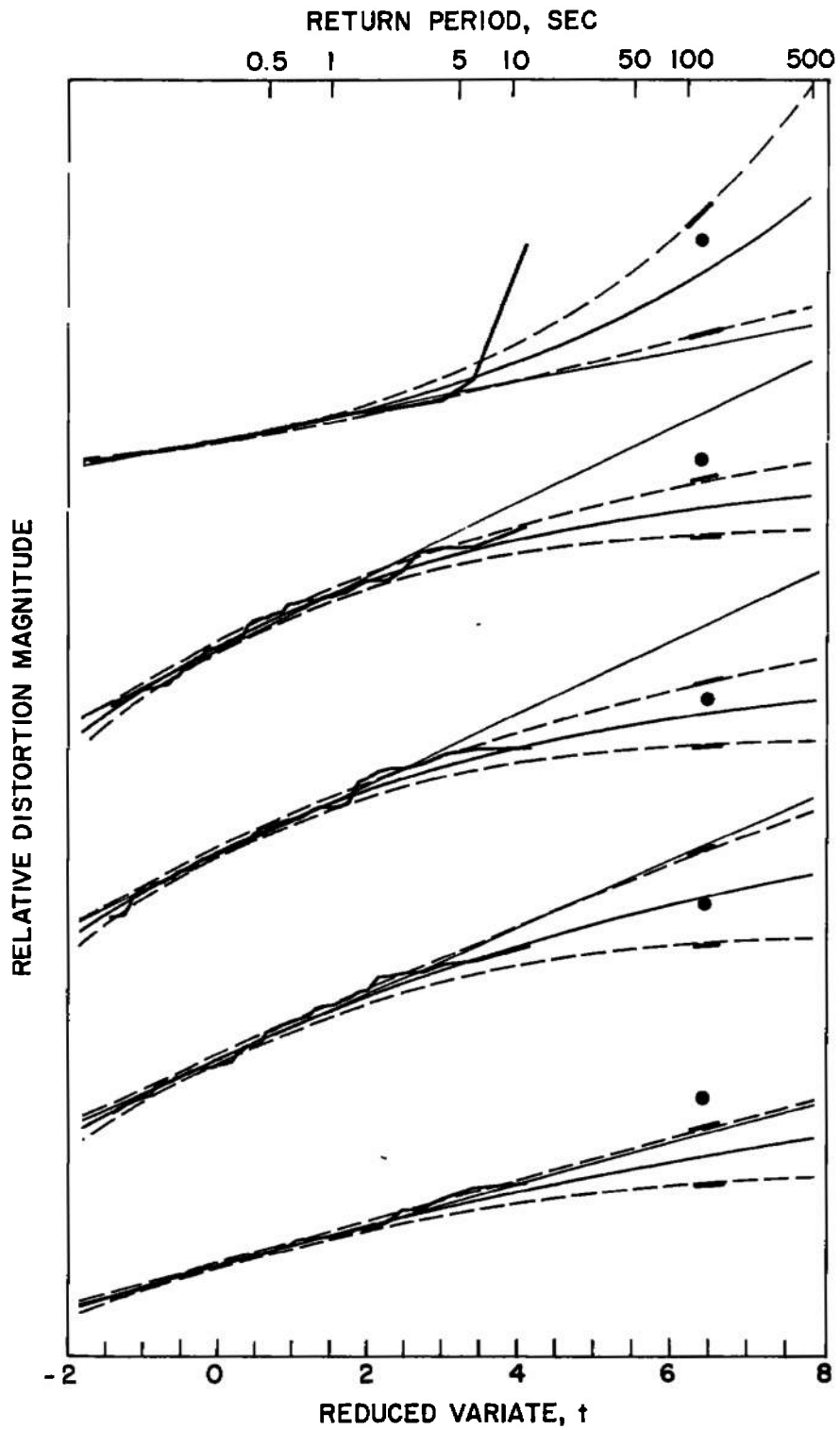


Figure 6. Continued.

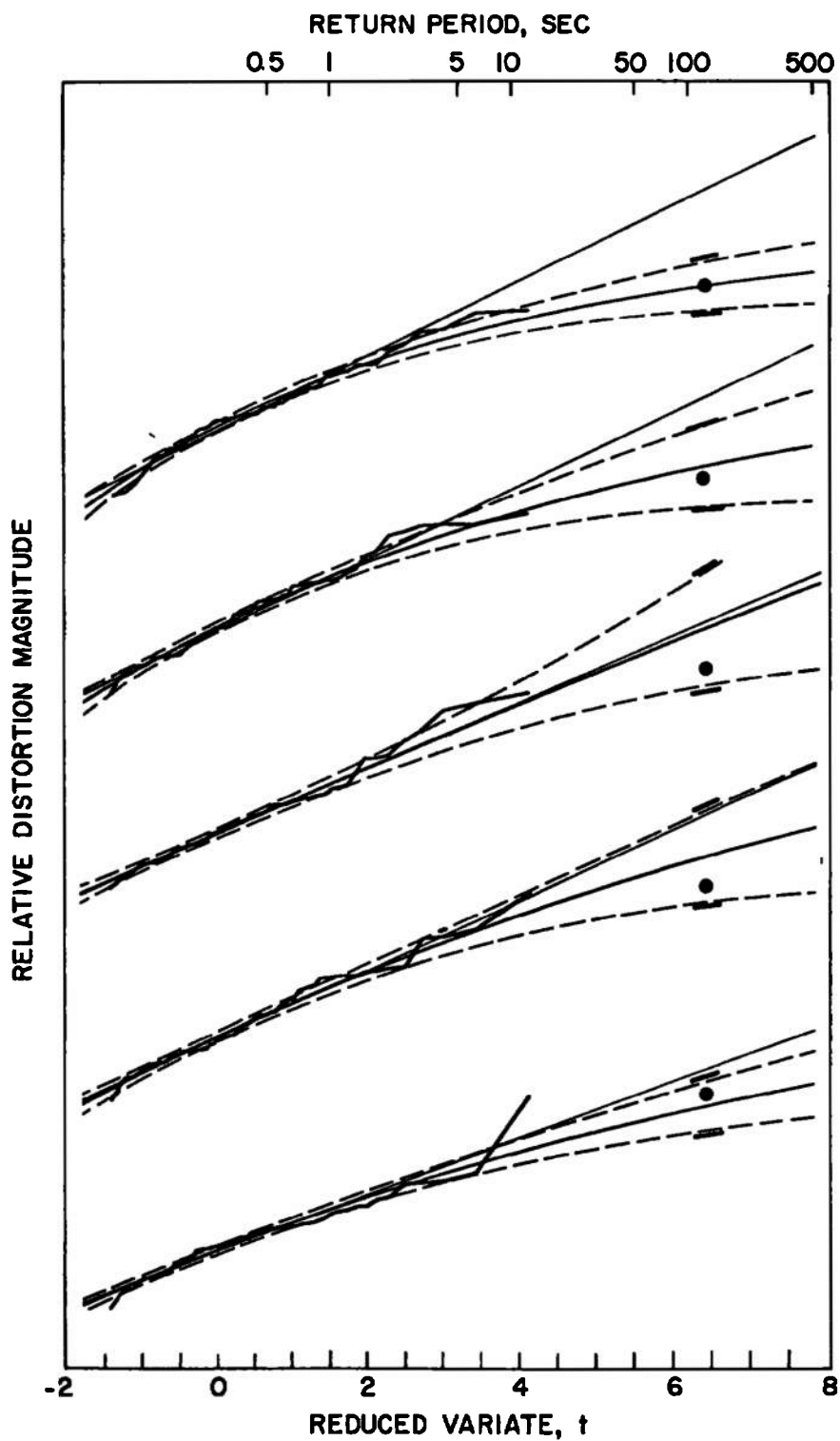


Figure 6. Continued.

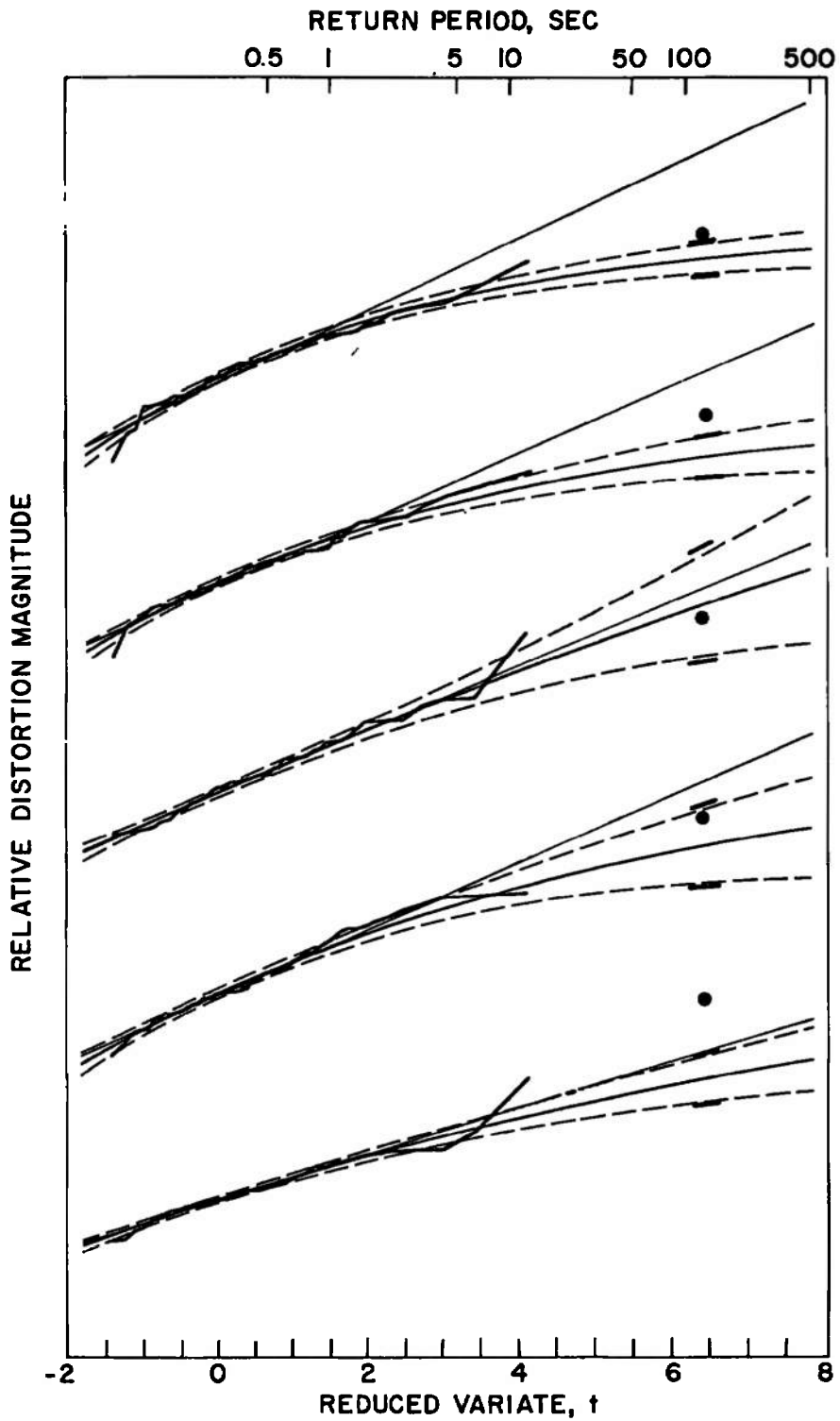


Figure 6. Continued.

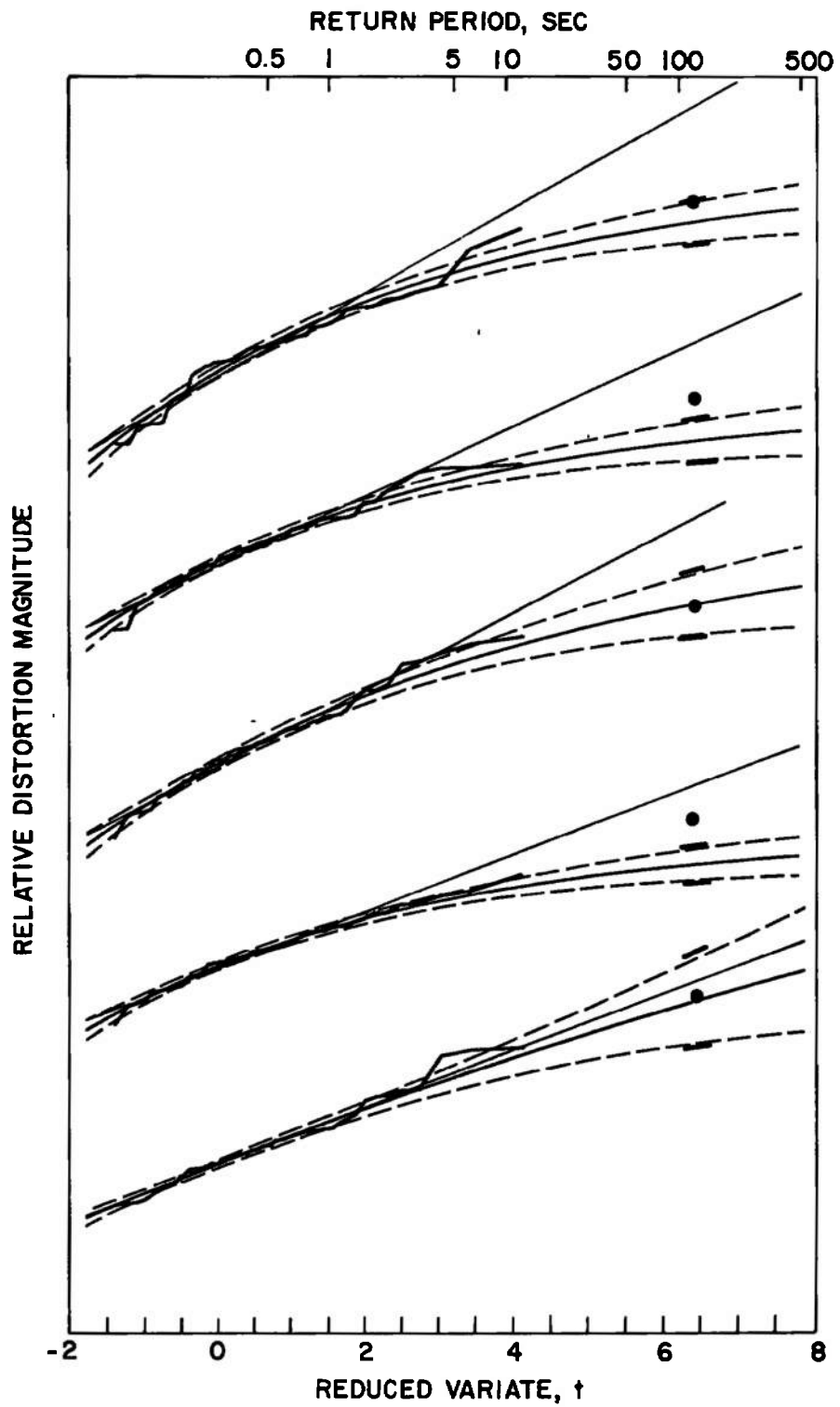


Figure 6. Concluded.

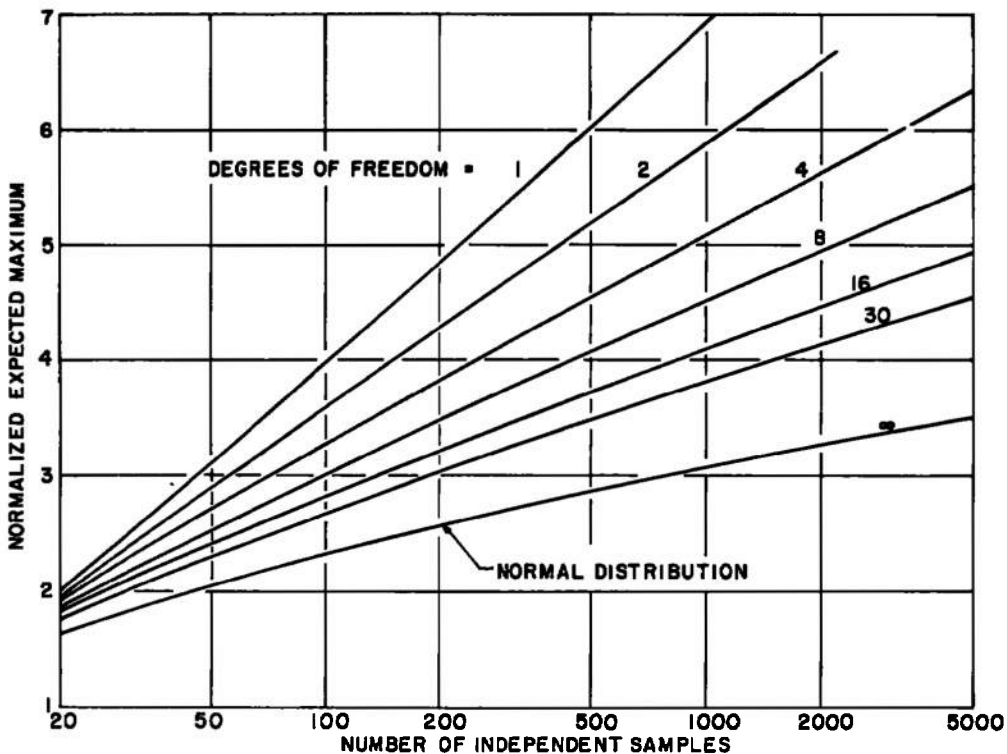


Figure 7. Dependence of the expected extreme on the number of independent samples for the Chi-square distribution family.

These results also point out the fallacy of the commonly used 3-sigma criteria for estimation of random variable maxima. Even if normality can be assumed, an expected maximum (or minimum) of three standard deviations away from the mean is valid only for nominally 1000 observations. The 3-sigma criteria are too stringent for a greater quantity of data and much too lax for fewer observations.

As further illustration of the effect of Δt variations, data from several test conditions similar to that used for Fig. 3 were processed, holding t constant at about 30 seconds and using nominal Δt increments of 0.1, 0.2, 0.4, etc. The dependence of the standardized modal value on the net number of extremes is given in Fig. 8 where each symbol corresponds to a specific test condition. The straight line fairings validate the expected logarithmic dependence of the mode on the number of extremes.

As with most statistical analyses, decreased confidence intervals are generally obtained with increased data quantity. On this basis, one would expect improved accuracy of the parameter estimates by maximizing the number of extremes selected. However, the

asymptotic theory of extreme values is not, in general*, valid for relative peaks that are comparable in magnitude to the mean of the total population, so that one must be careful to select extremes which are truly large. It is therefore recommended that each peak be selected from nominally 50 independent samples subject to a lower practical limit of 20 extremes altogether.

The incremental time Δt required to obtain 50 independent samples of distortion data depends on the inlet size (scale), turbulence level, and frequency bandwidths of the pressure signals and distortion calculator. Further, there appears to be some dependence on the nature of the turbulence with differing results being noted for simple boundary-layer radiated noise and the more regular shock-boundary-layer interaction turbulence generation, the latter requiring more data for independence.

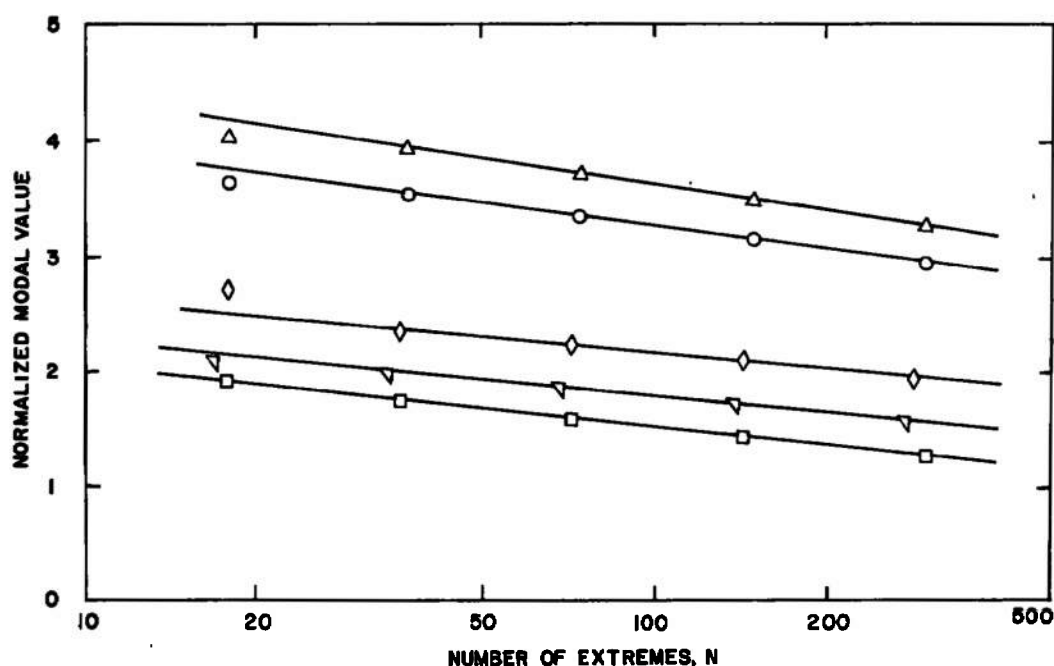


Figure 8. Dependence of the modal value on the number of extremes.

4.2 EFFECT OF FREQUENCY BANDWIDTH

Moore (Ref. 5) has developed the similarity parameter λ to correlate time-variant distortion data from various scale inlets, the expression being

*Of course, if the parent population distribution matches Eq. (5), then the asymptotic theory is valid for all observations.

$$\lambda \equiv \frac{2\pi r f_c}{a} \quad (12)$$

where

- r = engine-face duct radius
- f_c = low-pass filter cutoff frequency
- a = local speed of sound

The need for this parameter is evidenced by the wide variation of observed peak instantaneous distortion as a function of frequency bandwidth, typified by the data of Fig. 9. These data were originally digitized at 7700 samples/sec for one second with a 2000-Hz low-pass analog filter ($\lambda = 2.4$), then digitally filtered to achieve varying λ . The different test conditions are identified by consistent symbols for Figs. 9 through 13.

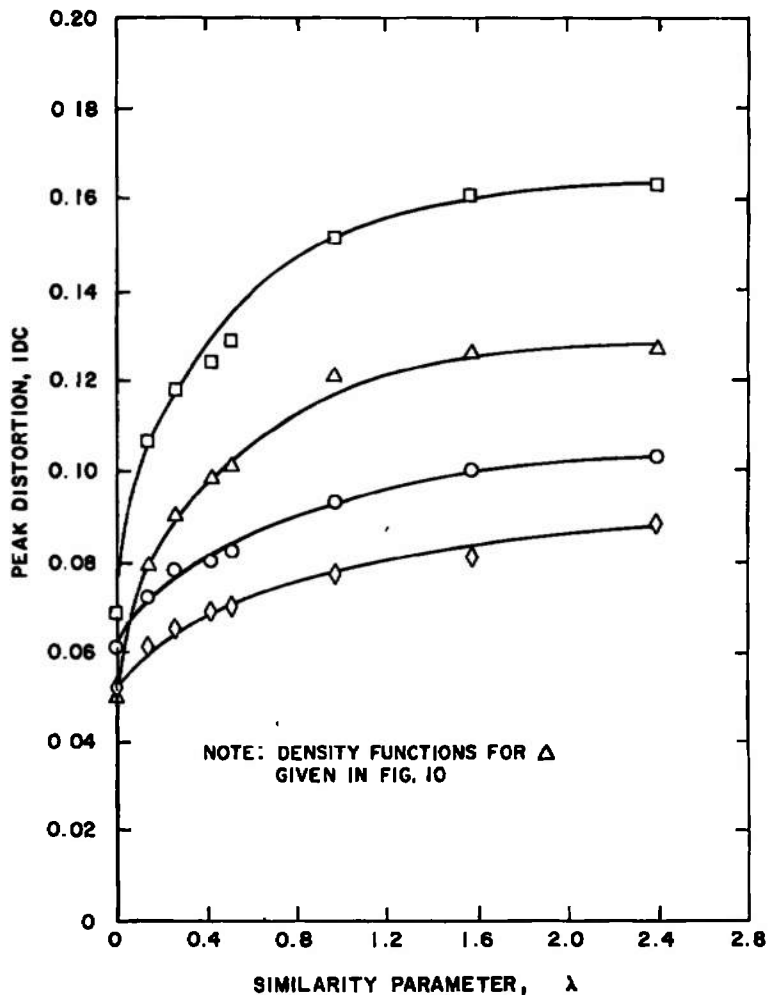


Figure 9. Effect of frequency bandwidth on peak distortion magnitude.

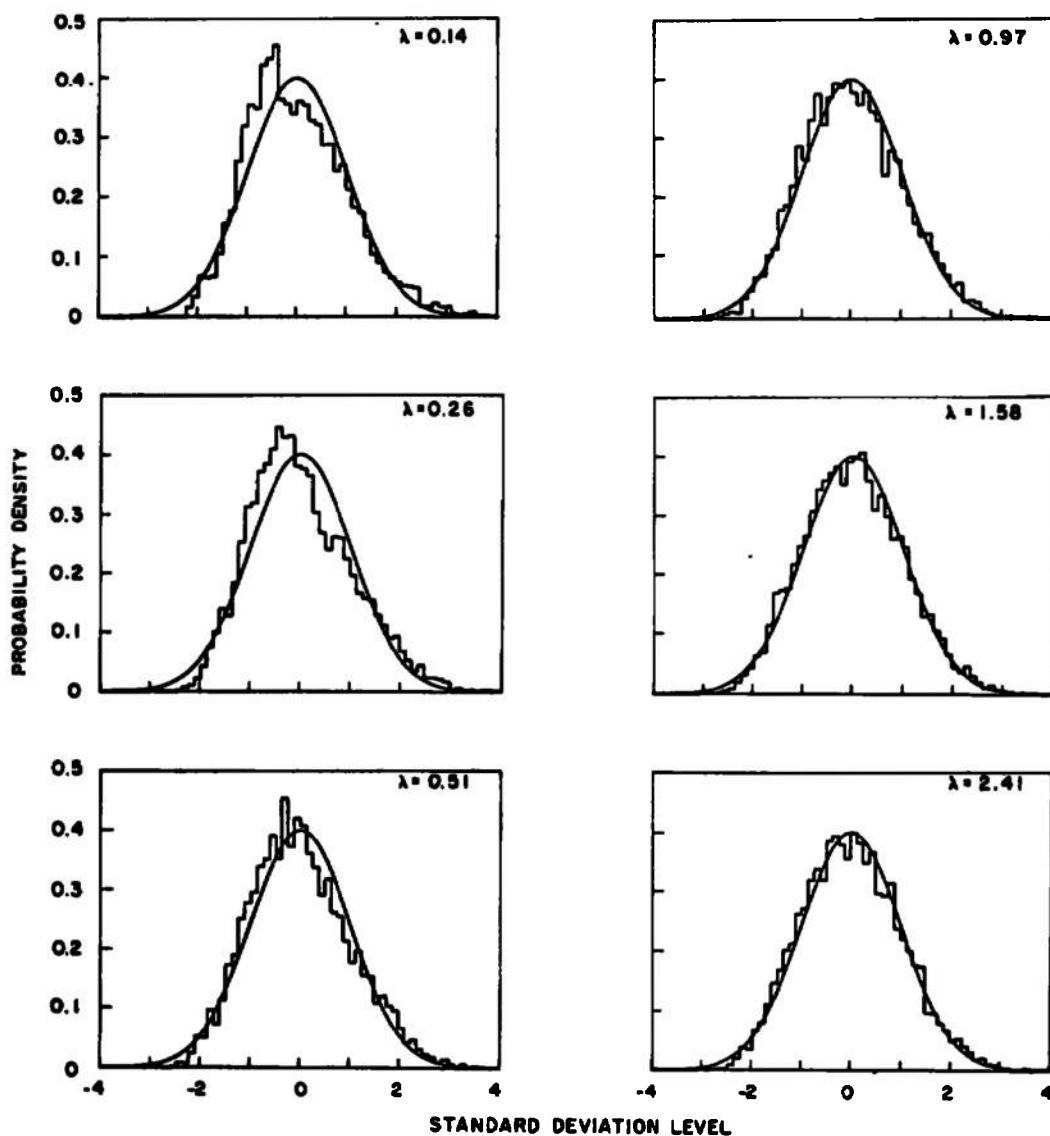


Figure 10. Computed probability density distributions with variation of Moore's similarity parameter.

Various engine manufacturers have settled on low-pass frequencies for time-variant distortion data analysis which nominally correspond to the engine rotation frequency, based on correlations of engine stalls with peak distortion data filtered at that frequency. For sonic tip speed, this frequency corresponds to $\lambda = 1$. The steady-state distortion level corresponds to $\lambda = 0$.

To gain insight as to the true effect of λ variations on distortion data, the probability density distributions for several test conditions were computed with a typical result given

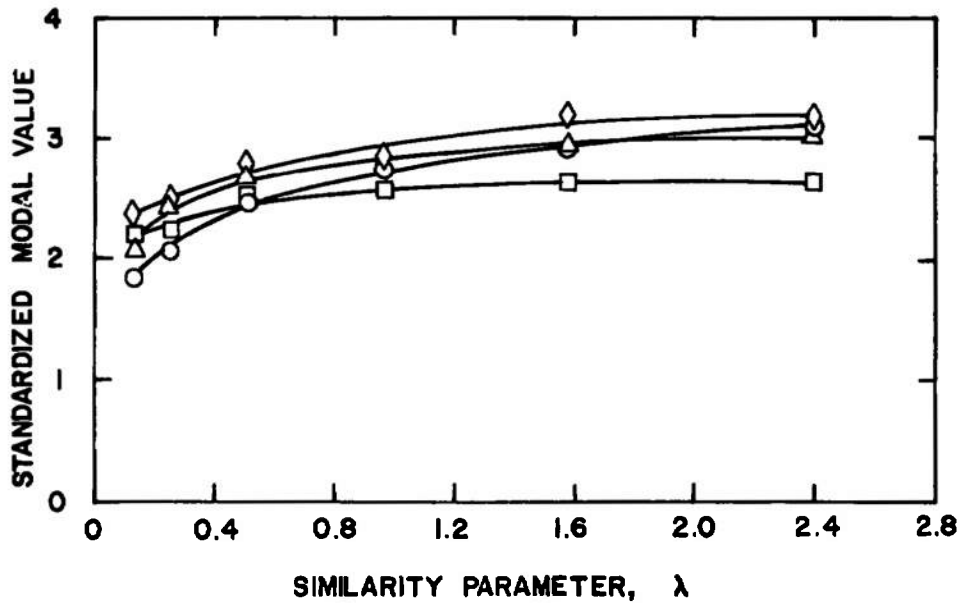


Figure 11. Effect of frequency bandwidth on the normalized modal distortion.

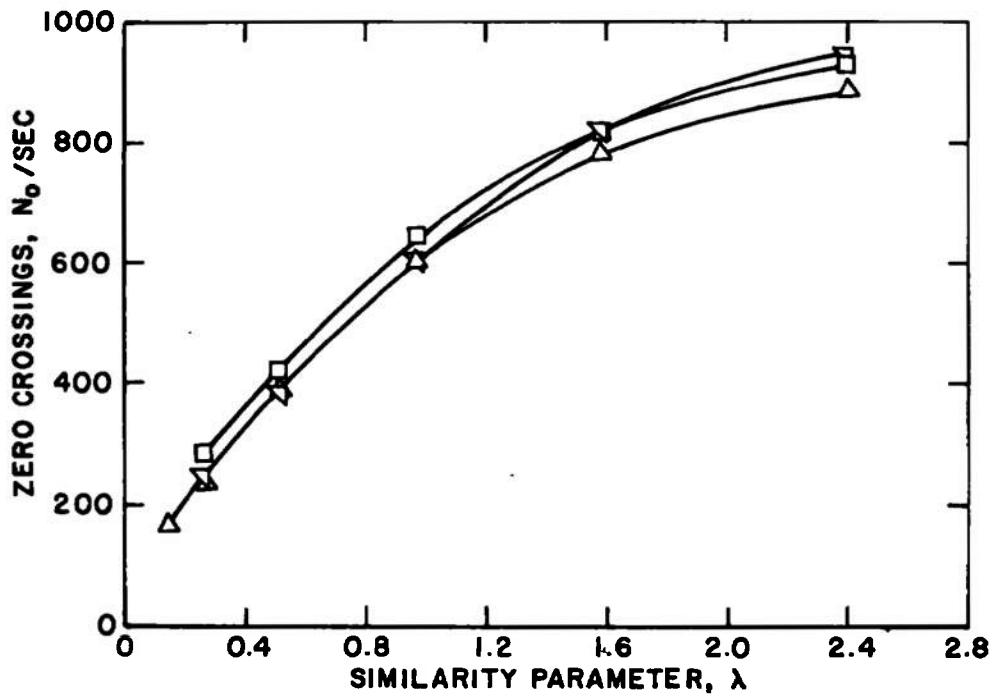


Figure 12. Effect of frequency bandwidth on the number of zero crossings.

as Fig. 10. Within the accuracy of these calculations, the probability density functions are reasonably independent of λ , although some skewness is evident. This independence is primarily the result of the rms level compensating for the variation in the data; that is, decreased frequency bandwidth yields decreased distortion fluctuation about a decreased mean (see footnote, Sec. 2.2), all being correlated by the usual standardized random variable. However, the extremes of distortion are not correlated by the rms level, there being a consistent trend of decreasing normalized peak distortion with decreasing λ . This trend is particularly evident (Fig. 11) for the modal value, the most frequently occurring distortion level.

Recalling Figs. 7 and 8, one way to observe a decreased expected extreme is for the number of independent samples to have decreased. Reference 12 offers a method* for estimating the number of zero crossings of a standardized random variable and this number is proportional to the number of effectively independent samples. The curvature of the normalized autocorrelation function, R , of the distortion factor at zero lag time, τ , is evaluated, with the number of zero crossings per second then given by

$$N_o = \frac{1}{2\pi} \left[- \frac{d^2 R}{d\tau^2} \right]_{\tau=0}^{1/2} \quad (13)$$

This parameter has been evaluated for a few test conditions with varying τ , the results being given as Fig. 12. Finally, Fig. 13 illustrates the modal value as a function of N_o/N along with the compatible result obtained by varying the number of independent samples per extreme by varying Δt as was done for Fig. 8. Thus, decreased frequency bandwidth results in both a decreased rms level and a reduction in the relative number of independent samples. Application of extreme-value statistics to time-variant distortion data therefore either requires consistent specification or compensation for any differences.

If λ is a true similarity parameter, then the effect of λ variation by means of frequency bandwidth variation is equivalent to variation by either the duct radius or the local sonic velocity. It is interesting to speculate that cold-day aircraft operation would be more conducive to engine stall than hot-day flights as a result of sound speed difference which causes higher peak distortion levels. It is known that variation of the duct radius must be compensated by changes in the filter frequency to achieve comparable distortion results.

*Although the method was developed assuming normally distributed data, it is used here with the results demonstrating its validity.

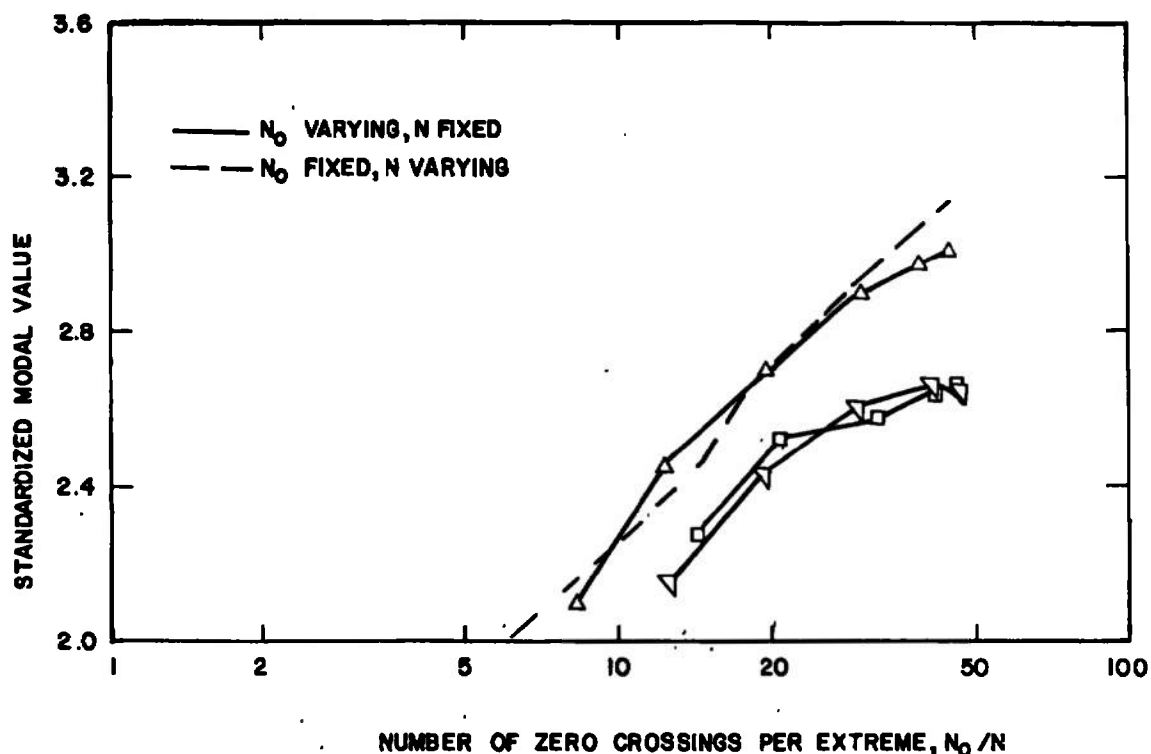


Figure 13. Dependence of the normalized modal distortion on the ratio of zero crossings to number of extremes.

5.0 RECOMMENDED PROCEDURES FOR ANALYSIS OF INLET DISTORTION

5.1 INLET DEVELOPMENT TESTING

Inlet performance is characterized by airflow, recovery, drag, and distortion. The ideal performance is that combination of high recovery, low drag, and low distortion, all at the desired engine-match airflow with a wide operating envelope about that match point. Real inlets are required to give acceptable performance over such a wide range of Mach number and aircraft attitude with resulting design compromises that the ideal performance level is rarely achieved for any operating condition. To monitor the effects of inlet modifications, several critical or representative conditions are selected and these "tracking points" then artificially become the most important test conditions.

Based on analyses of time-variant inlet distortion data from four aircraft designs and observations of the airframe and engine manufacturers' profitable use of wind tunnel test data on sub-scale and full-scale inlet models, the following procedures are recommended:

1. The current practice for data acquisition is to record the time-variant engine-face total-pressure signals for 30 seconds at each test condition for a sub-scale model inlet test. This time period is necessary to be reasonably sure of documenting the higher distortion levels, particularly so if one is seeking a representative peak instantaneous distortion. However, since application of extreme-value statistics to a short (1 to 2 seconds) data segment can yield equivalent results, it is recommended that data acquisition times be correspondingly reduced. Verification of the validity of the extreme-value analysis can be accomplished by optionally testing longer at the tracking points. It is suggested that a data acquisition time period equivalent to 5 sec of full-scale inlet operation is sufficient to document the statistical characteristics of inlet flowfields at stationary test conditions.

2. The distortion factor time series can be obtained from analog and/or digital computers, specific examples are discussed in Section 5.3. Whatever the means, it is recommended that the entire time period be processed to obtain the distortion extremes with analysis as discussed herein.

3. Since the results to be obtained from the extreme-value analysis are dependent on the data time base, it is important that this time base be held fixed throughout a test series. In like manner, the similarity parameter λ must be maintained constant to achieve comparable results. The final parameter to be selected is the number of extremes, N . Based on the analyses conducted during preparation of this report, it is recommended that $N = 30$ be used for normal data processing.

4. It is recommended that the parameters of both the first and general asymptotes be evaluated for reasons discussed in Section 5.3. The end result should be an estimation of the expected maximum distortion level (with tolerance band) to be encountered within a specific time interval of full scale inlet operation.

5. Inlet design optimization cycles would then be targeted towards reducing this distortion level without compromising other performance criteria. If the indicated distortion reduction lies within the tolerance band, then one should not conclude that that particular optimization path had significant influence on maximum time-variant distortion levels.

5.2 INLET/ENGINE COMPATIBILITY DEMONSTRATION

As discussed in Section 2.2, distortion patterns for screen simulation of inlet flow should be based on the steady-state pattern rather than on one isolated instantaneous pattern. The extreme-value analyses can be used to determine the desired intensification of the steady-state distortion level, based on the return period concept.

The available stall margin is usually allocated to engine tolerances, age deterioration, transients, and distortion, with all of these assumed to be additive. It is suggested that some blending of the allocation for transients and distortion is proper in that the expected distortion maximum within the time duration of a transient is significantly less than that associated with steady-state operation.

Conversely, the distortion level selected for engine qualification should be representative of that expected within the time period of the simulated flight condition. That is, the distortion level should correspond to that expected in a period of hours for a cruise condition but perhaps only seconds for a maneuver condition.

Engine testing with an inlet or inlet simulator is the true proof of inlet/engine compatibility. For this type of testing, one is not interested in the distortion levels which could occur but rather what did occur. Extreme-value analysis of the time-variant distortion is still beneficial in the sense of data quality assurance and detection of abnormal flow conditions. An engine stall may occur as the result of an instantaneous peak distortion level which would be expected only once during the engine's lifetime; demonstrated stall-free engine operation for this event is a criteria too stringent for normal inlet/engine compatibility testing.

5.3 DATA PROCESSING

The mechanics of obtaining the distortion extremes depend on the resources available, such as analog and/or digital computers and capability for time-correlated analog-to-digital signal conversion of the engine-face pressures. Various techniques were used for the illustrations contained herein and a discussion of these procedures is given below, followed by a description of an "ideal" system.

The analysis illustrated by Fig. 3 was based on the availability of an analog computer which calculated various distortion factors in real time, the output being recorded in analog form on magnetic tape. Subsequently, the distortion factor signal was played back through a peak detector with the detector threshold being reset every 0.1 sec after the output level was read by an analog-to-digital data acquisition system. The digital distortion extremes were then recorded on magnetic tape for later analysis.

The data contained in Fig. 4, representing 28 seconds of inlet operation, were obtained in the manner given above, except that the peak detection and digitizing were accomplished in real time in conjunction with an on-line data acquisition system. The data representing one second of inlet operation were obtained subsequently by digitizing the engine-face pressure signals (time selected at random), digitally computing the distortion factor at each time slice, and then selecting the extreme from each of twenty equal time intervals.

Although no examples are contained herein, many segments of digital pressure signals for a short time interval containing the instant of peak distortion from a much longer time period have been processed. Direct application of extreme-value statistics is possible provided one weights the largest distortion peak according to the corresponding time ratios (and assumes the second largest peak is independent of the first).

The data of Figs. 5 and 6 and analysis results were obtained in practically real time by monitoring the output of an analog computer with a peak detector resetting every 0.2 seconds for a total of 12 seconds. The analog computer also contained a peak detector which was not reset, so that at the conclusion of the data acquisition time period of nominally two minutes the peak instantaneous distortion level was also available. The 12-second set of extremes was then digitally processed to obtain the results shown with the analysis being a part of the on-line test data package.

The major shortcomings of an analog distortion calculator is the unavoidable inaccuracy created by the approximations used to compute a distortion factor and by the inability to compensate for zero shifts of the dynamic transducers. Although these difficulties can be overcome with digital processing, the expense and time required are prohibitive for most test conditions. However, it is feasible to combine the features of the two techniques into a hybrid analog/digital system which would provide digital processing accuracy at nominally analog processing expense. The technique would consist of monitoring the analog distortion signal with a peak detector, sample and hold the individual pressure signals at the instant of each step in the peak detector output, digitize the stored pressure data at fixed time intervals, transfer this information to digital computer memory, and then reset the peak detector and continue. If measurements of the true steady-state pressure and time-averaged outputs of the dynamic transducers are available, then the differences are the zero shifts which can be applied to the instantaneous pressure data and the distortion extremes thence computed without error.

The analyses presented as Fig. 6 include some examples of the distortion data indicating the second asymptote to be the best descriptor (curved up instead of down). This occurrence is attributed to sampling fluctuation. In such cases it is recommended that the first asymptote be used instead of the general results and the answers flagged accordingly.

The use of maximum likelihood estimation for the parameters necessitates utilization of a digital computer to obtain the results. A FORTRAN listing of the program developed for this purpose is given in Appendix C along with samples of input/output. The various subroutines have not been optimized from the standpoint of computer time so that execution time (including plotting) averages about 3 seconds for 60 extremes on an IBM System 370/155, required core being about 70k dependent on the data sources(s). A card deck is available on request to the authors.

6.0 CONCLUDING REMARKS

Application of Gumbel's extreme-value statistics analyses to time-variant inlet data from four aircraft designs has led to the following results and recommendations:

1. The peak instantaneous distortion as observed within a finite data acquisition time period is random and not repeatable, as is the engine-face pressure pattern for that instant.
2. A short time segment of distortion data can be used to statistically predict the expected maximum distortion level corresponding to any time period of inlet operation, including estimates of the prediction tolerance.
3. Engine qualification testing should use screens based on the steady state rather than a peak instantaneous distortion pressure pattern with the distortion being intensified to the expected maximum level corresponding to the aircraft operation time at specific test conditions.
4. Data acquisition time periods during inlet development wind tunnel testing can be reduced from the current 30 seconds to nominally 2 seconds for stationary test conditions, provided that analysis of the resulting time-variant distortion is based on extreme-value statistics.

REFERENCES

1. Jacocks, J. L. "Statistical Analysis of Distortion Factors." AIAA Paper No. 72-1100, Presented at AIAA/SAE 8th Joint Propulsion Specialist Conference, New Orleans, Louisiana, November 29 - December 1, 1972.
2. Gumbel, E. J. Statistics of Extremes. Columbia University Press, New York, 1958.
3. Hald, A. Statistical Theory with Engineering Applications. John Wiley and Sons, Inc., New York, 1952.
4. Hartley, H. O. "The Modified Gauss-Newton Method for the Fitting of Non-Linear Regression Functions by Least Squares." *Technometrics*, Vol. 3, No. 2, May 1961, pp. 269-280.
5. Moore, Michael T. "Distortion Data Analysis." General Electric Company, AFAPL-TR-72-111 (AD756481), February 1973.

6. Kimzey, W. F. and Lewis, R. J. "An Experimental Investigation of the Effects of Shock-Induced Turbulent In-Flow on a Turbojet Engine." Paper Presented at the AIAA 2nd Propulsion Joint Specialist Conference, United States Air Force Academy, Colorado Springs, Colorado, June 13-17, 1966.
7. Rall, F. T. "Aircraft and Propulsion Operational Considerations Related to Inlet Design." Paper No. 5 of "Integration of Propulsion Systems in Airframes." AGARD Conference Proceedings No. 27, September 1967.
8. Hoeflinger, R. F. "Diffused Diaphragm Pressure Sensors and Impact Probes." ISA Paper 69-672, Advances in Instrumentation, Vol. 24, Part IV, 1969, Proceedings of the 24th Annual ISA Conference, Houston, Texas, October 27-30, 1969.
9. Crites, Roger C. "The Philosophy of Analog Techniques Applied to the Analysis and High-Speed Screening of Dynamic Data." AIAA Paper No. 70-595, May 1970.
10. Kimzey, W. F. and McIlveen, M. W. "Analysis and Synthesis of Distorted and Unsteady Turboengine Inlet Flow Fields." AIAA Paper No. 71-668, Presented at AIAA Seventh Propulsion Joint Specialist Conference, Salt Lake City, Utah, June 14-18, 1971.
11. Abramowitz, M. and Stegun, I. A. "Handbook of Mathematical Functions with Formulas, Graphs, and Mathematical Tables." National Bureau of Standards Applied Mathematics Series No. 55, June 1964.
12. Bendat, Julius S. "Probability Functions for Random Responses: Prediction of Peaks, Fatigue Damage, and Catastrophic Failures." NASA CR-33, April 1964.
13. Burcham, Frank W., Jr., Hughes, Donald L., and Holzman, Jon K. "Steady-State and Dynamic Pressure Phenomena in the Propulsion System of an F-111A Airplane." NASA TN D-7328, July 1973.
14. Mood, A. M. Introduction to the Theory of Statistics. McGraw-Hill Book Company, Inc., New York, 1950.

APPENDIX A

DISTORTION FACTOR FORMULATIONS

Complete description of the engine-face total-pressure pattern requires specification of all the pressure measurements, P , which make up that pattern (a difficult comprehension task when dealing with forty or so measurements). Various investigators have attempted to quantify the significant characteristics of the patterns with a manageable set of descriptors, termed distortion factors, which describe both the nature and intensity of nonuniformity.

The distortion factors have evolved from the simple expressions:

$$D_1 = \frac{(\text{maximum } P - \text{minimum } P)}{\text{average } P}$$

and

$$D_2 = \frac{(\text{average } P - \text{minimum } P)}{\text{average } P}$$

which specify the intensity or magnitude of distortion through slightly more complicated expressions which distinguish between radial and circumferential variation in the total pressure to the current methodologies of Pratt and Whitney or General Electric, for example, which correlate engine stall margin with distortion level.

The specific distortion factor equations used for the current study are given herein for the purpose of illustrating both the differences among them and an overall sameness when considered as descriptors of a stochastic process. Even though the distortion factor formulations vary considerably, the resultant time-variant description of inlet flow nonuniformity is basically random and, when normalized by the mean and standard deviation of the time series, notable consistency is achieved with the extreme-value statistics.

PRATT AND WHITNEY DISTORTION FACTORS (Ref. 13)

Referring to Fig. A-1 for the general engine-face probe geometry and nomenclature, the measured pressures are designated by P_{ij} with i being the ring designation and j denoting the rake location. The circumferential distortion factor, KTH, is computed by obtaining a 4-term Fourier fit to each ring of pressures

$$P_i(\theta_j) = \frac{1}{J} \sum_{j=1}^J P_{ij} + \sum_{n=1}^4 A_n \sin(n\theta_j + \phi)$$

and selecting the maximum weighted harmonic amplitude for each ring

$$A_i = \text{maximum } (A_{ni}/n^2)$$

KTH is then given as

$$KTH = \frac{\sum_{i=1}^I A_i/D_i}{q \sum_{i=1}^I 1/D_i}$$

where q = face-averaged dynamic $(1/2 \rho v^2)$ pressure.

The radial distortion factor, KRA, is normally computed as a weighted average of deviations in average ring pressure from a base or reference radial profile. For the current study the reference profile was uniform with KRA being computed from

$$KRA = \frac{\sum_{i=1}^I \left| \frac{1}{J} \sum_{j=1}^J P_{ij}/\bar{P} - 1 \right| D_i^{-n}}{q/\bar{P} \sum_{i=1}^I D_i^{-n}}$$

where \bar{P} = face-averaged pressure

n = radial weighting exponent = 2.86

The face-distortion factor KA2 is computed as a weighted sum of the circumferential and radial components:

$$KA2 = KTH + b KRA$$

where b = weighting function.

For most test conditions and most inlets, the radial and circumferential components are negatively correlated, with one result being that the peak or maximum instantaneous KA2 is less than the weighted sum of the component peaks.

GENERAL ELECTRIC DISTORTION FACTORS (Ref. 5)

The circumferential parameter, IDC, and the radial parameter, IDR, are both dependent on ring-averaged pressures

$$R_i = \frac{1}{J} \sum_{j=1}^J P_{ij}$$

For each ring, the lowest pressure in the ring defines an IDC component

$$IDC_i = (R_i - P_{ij \min})/\bar{P}$$

thence, hub and tip parameters are computed as the average of the two ring components

$$IDC_{hub} = (IDC_1 + IDC_2)/2$$

$$IDC_{tip} = (IDC_I + IDC_{I-1})/2$$

and then the circumferential distortion factor is assigned the magnitude of the largest component

$$IDC = \text{maximum of } IDC_{hub} \text{ or } IDC_{tip}$$

The radial distortion components in each ring are defined as

$$IDR_i = (\bar{P} - R_i)/\bar{P}$$

and the radial distortion factor is assigned the magnitude of the largest of the hub and tip components

$$IDR = \text{maximum of } IDR_i; i = 1, 2, I-1, I$$

An overall distortion factor ID can be expressed as simply

$$ID = IDC + IDR$$

but the more descriptive stall margin parameter can be computed from the components of the circumferential and radial distortion parameters utilizing extent and shape parameters. Some data presented herein were computed using nominal stability usage factors, B , in the form

$$IDL = B_c \times IDC + B_R \times IDR$$

To illustrate the statistical similarity of all these distortion factors, one segment of digital time-variant engine-face data was processed with all distortion factors being computed. Results of application of the order statistics are given in Fig. A-2 with the ordinate being the normalized parameters, that is, subtracting the mean value and dividing by the standard deviation of the basic distortion factor time series. The basic point to be made is that any distortion factor computed from time-variant engine-face pressures can be treated as a random variable. Practically regardless of the formulation of that distortion factor, the underlying pressure data govern the characteristics of the result and, in particular, control the probability distribution of the extremes.

As noted in the text, the time-variant distortion factors are calculated by both analog and digital computers. The accuracy of the analog results from four representative inlet tests has been evaluated by also processing data digitally around the time of the peak instantaneous distortion. These data are given in Fig. A-3 and show the analog computers to be typically about five-percent accurate. However, later designs utilizing hybrid analog/digital processing have demonstrated one-percent accuracy.

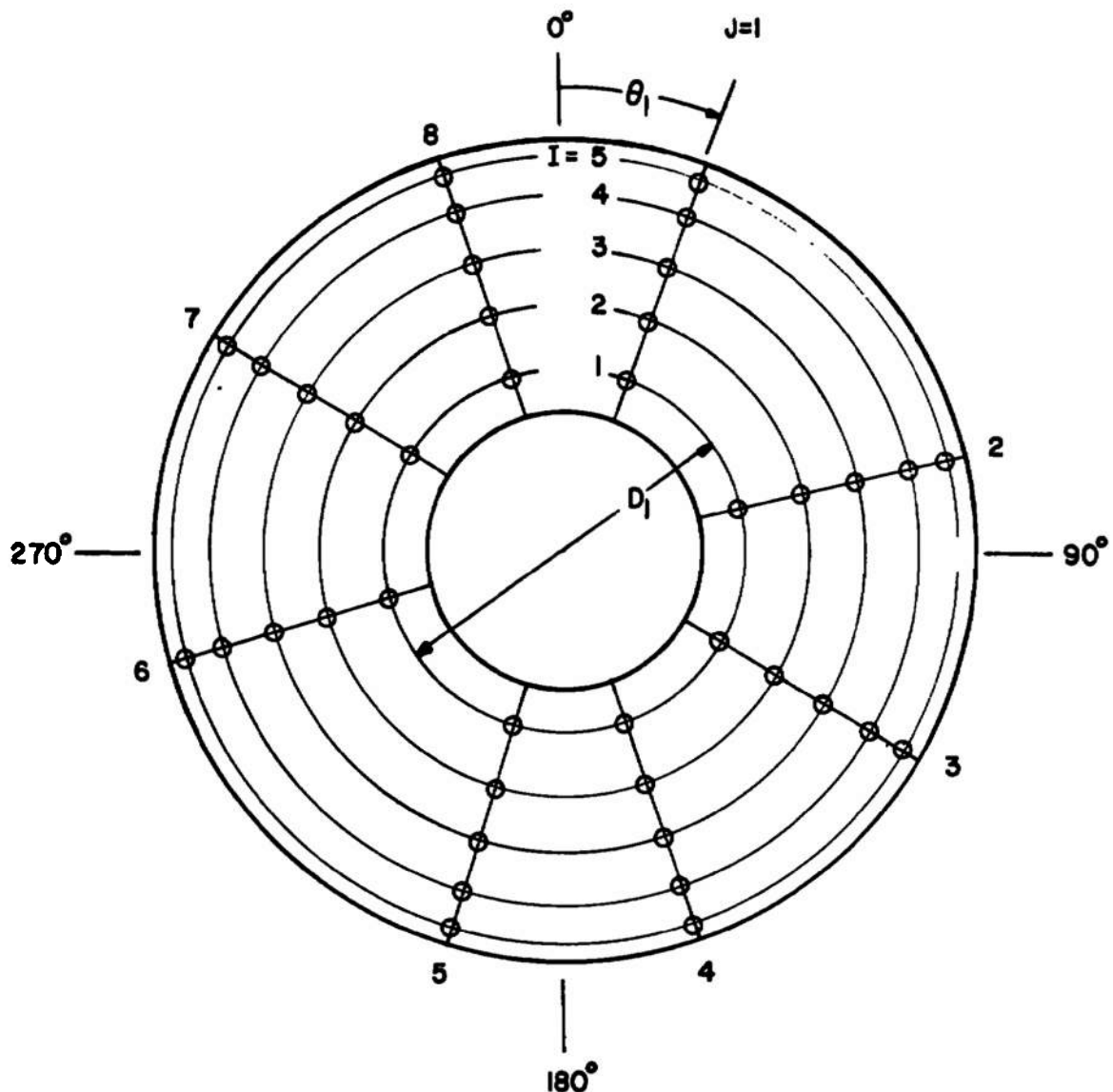


Figure A-1. General engine-face probe geometry and nomenclature.

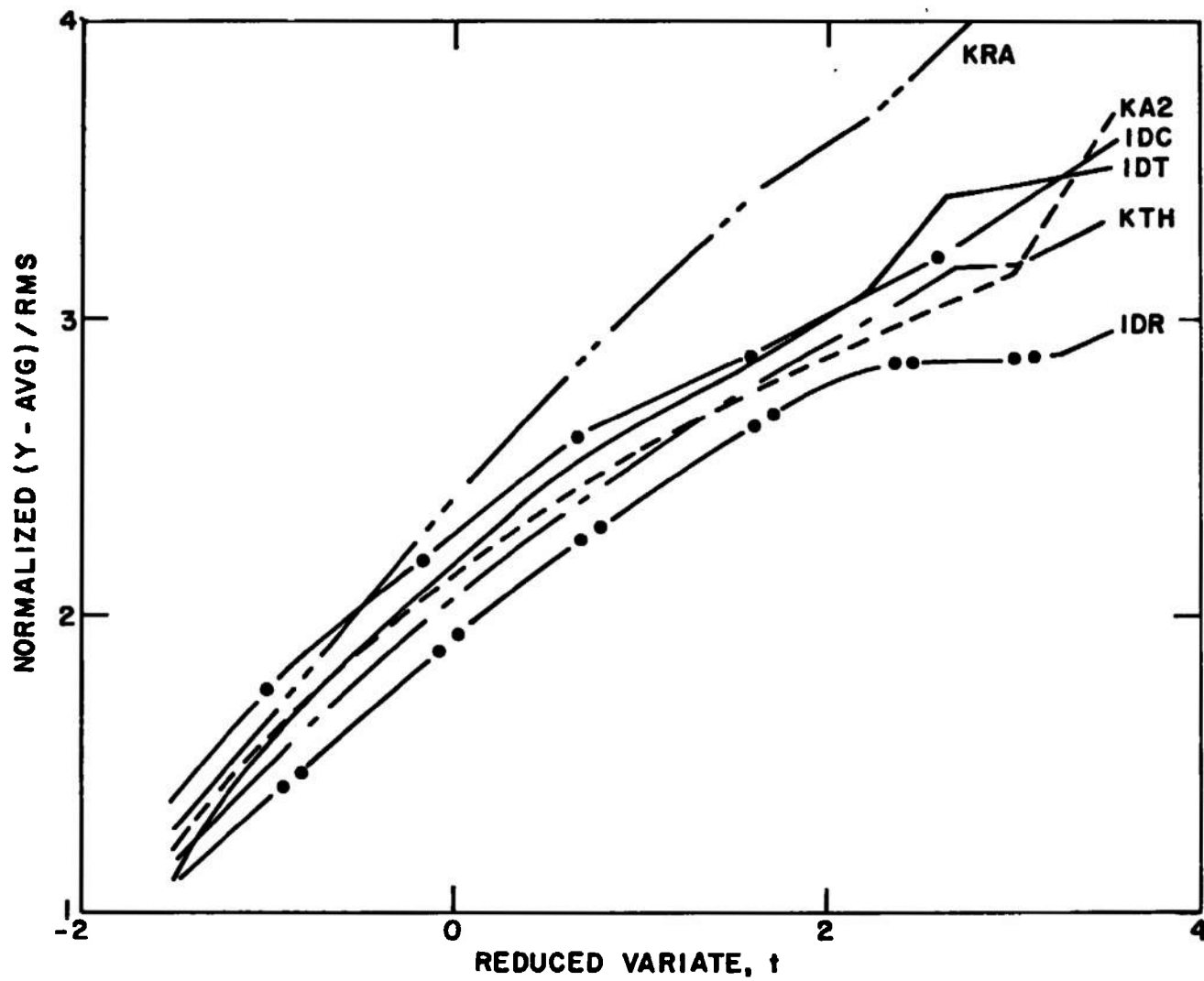


Figure A-1. Comparisons of the cumulative distribution of various distortion factors.

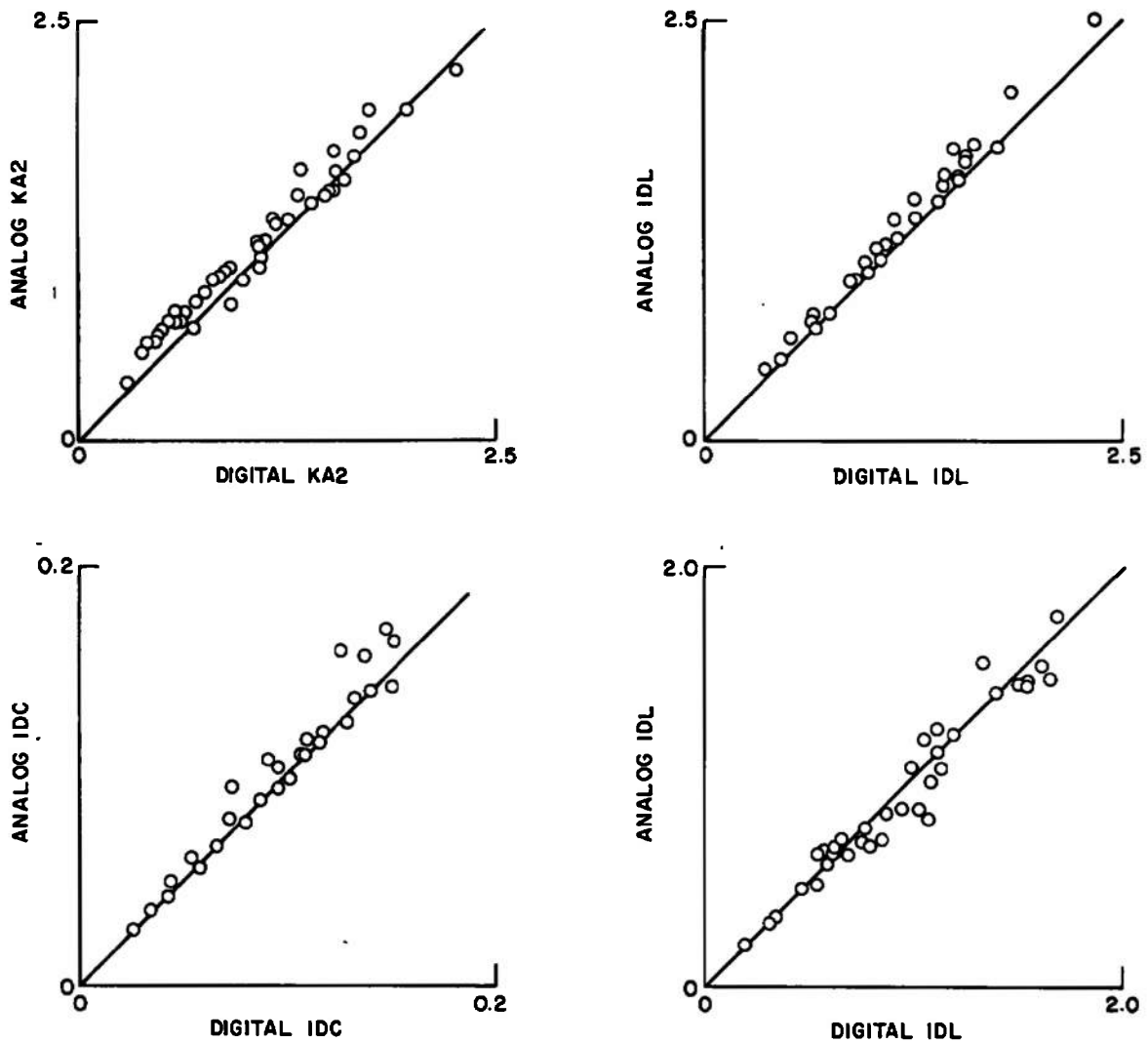


Figure A-3. Evaluation of the accuracy of analog distortion computers.

APPENDIX B ANALYTIC DETAILS

The objective of this Appendix is to provide the necessary supportive background for interpretation and application of Gumbel's asymptotic theory of extreme values. The generalized three-parameter distribution is formed from the third asymptote, followed by a discussion of its properties with respect to independent sampling and sampling from different time interval lengths. Details of the parameter estimation procedure are given, including the method of variance approximation.

As a starting point, consider

$$Y = \text{maximum } (y_i) \text{ } i = 1, 2, \dots, n$$

where the y_i are identically distributed independent random variables. As shown by Gumbel (Ref. 2), the asymptotic distribution of Y as n increases depends upon the distribution of the individual y , with three specific types of parent distributions yielding Gumbel's three asymptotes.

Exponential type (First Asymptotic Distribution):

$$F(y) = \exp [-\exp [-a_1 (y - a_2)]] \quad (B-1)$$

Cauchy type (Second Asymptotic Distribution):

$$F(y) = \exp [-(b_1/y)^{b_2}] \quad (B-2)$$

Limited type (Third Asymptotic Distribution):

$$F(y) = \exp \left[-\frac{c_2 - y}{c_2 - c_1} \right]^{c_3} \quad (B-3)$$

where a_i , b_i , and c_i are parameters. All three asymptotes can be expressed by a generalized three-parameter distribution by substituting into Eq. (B-3):

$$a = c_2/c_3$$

$$\beta = 1/c_3$$

$$\nu = c_1$$

with the result being

$$F(y) = \exp \left[- \frac{a - \beta y}{a - \beta \nu} \right]^{1/\beta} \quad (\text{B-4})$$

$$F(y) = 0 \quad y \leq a/\beta \text{ and } \beta < 0$$

$$F(y) = 1 \quad y \geq a/\beta \text{ and } \beta > 0$$

The first asymptote results from Eq. (B-4) with $\beta = 0$, the second asymptote in three-parameter form with $\beta < 0$, and the third asymptote with $\beta > 0$.

Two important properties of the generalized asymptote $F(y; a, \beta, \nu)$ are: (1) the distribution of Y may be made arbitrarily close to some distribution from the $F(y; a, \beta, \nu)$ family by choosing a sufficiently large n . The distribution chosen from $F(y; a, \beta, \nu)$ as being approximately equal to the distribution of Y will depend upon n , in which case the parameters should be subscripted, (a_n, β_n, ν_n) ; and (2) if the distribution of the y_i is a member of $F(y; a, \beta, \nu)$, then the distribution of Y is a member of $F(y; a, \beta, \nu)$ for all n .

Let us now turn to the real problem of a stochastic process $x(t)$ wherein we seek the distribution of X which is composed of the maximum of $x_i(t)$, ($i = 1, 2, \dots, n$) selected from sub-time intervals Δt . It is assumed that the process is stationary and ergodic so that the x_i are identically distributed, but they are not independent. However, though adjacent values of $x(t)$ may show strong correlation it is not unreasonable to assume that two values are essentially independent if they are separated by a sufficiently large time interval τ . Following this line of reasoning, an interval of size $n\Delta t$ would contain $n\Delta t/\tau$ independent samples. If $n\Delta t \gg \tau$ then one could conclude the distribution of X is describable by the asymptotic distribution $F(x; a, \beta, \nu)$. While these comments are heuristic, the conclusion has been rigorously shown for certain cases and assumptions (Ref. 2). An even better justification for the implied assumptions of independence of the $x_i(t)$ is the excellent results obtained when using actual distortion data. As with the independent case where the parameters a , β , and ν depend upon n , in the case of a stochastic process these parameters are functionally dependent upon the interval size $n\Delta t$.

This interval size dependence can be shown by postulating X_i to be the maximum of i^{th} of n adjoining intervals, such that the maximum X^* of these X_i may also be considered to be the maximum of an interval n times in size. The multiplication rule yields

$$F_{X^*}(x; a_n, \beta_n, \nu_n) = F_{X_i}(x; a, \beta, \nu)$$

Now consider x_{T_1} and x_{T_2} to be maximums from intervals of lengths T_1 and T_2 , respectively. If T_1 and T_2 are commensurate, then we can write

$$\frac{T_2}{T_1} = \frac{m}{n} = r$$

where m and n are integers. Let x_{T_3} be the maximum from an interval of length mT_1 or nT_2 , then

$$\begin{aligned} F_{x_{T_3}}(x; a, \beta, \nu) &= F_{x_{T_1}}^m(x; a_{T_1}, \beta_{T_1}, \nu_{T_1}) \\ &= F_{x_{T_2}}^n(x; a_{T_2}, \beta_{T_2}, \nu_{T_2}) \end{aligned}$$

or

$$F_{x_{T_2}}(x; a_{T_2}, \beta_{T_2}, \nu_{T_2}) = F_{x_{T_1}}^r(x; a_{T_1}, \beta_{T_1}, \nu_{T_1})$$

The incommensurate cases follow if $F_{x_{T_2}}$ is assumed to be a continuous function of r . Substituting the above into (B-4) yields

$$\left[\frac{a_{T_2} - \beta_{T_2} x}{a_{T_2} - \beta_{T_2} \nu_{T_2}} \right]^{1/\beta_{T_2}} = r \left[\frac{a_{T_1} - \beta_{T_1} x}{a_{T_1} - \beta_{T_1} \nu_{T_1}} \right]^{1/\beta_{T_1}}$$

This being an identity for all x implies

$$a_{T_2} = a_{T_1}$$

$$\beta_{T_2} = \beta_{T_1} \tag{B-5}$$

$$\nu_{T_2} = \frac{1}{\beta_{T_1}} \left[a_{T_1} - (a_{T_1} - \beta_{T_1} \nu_{T_1}) r^{\beta_{T_1}} \right]$$

Thus the parameters a and β are independent of interval size and, for $\beta \geq 0$, the parameter ν is a monotonic increasing function of the interval size for fixed frequency bandwidth. This effect must be considered when comparing probability plots of data where the interval sizes are different. Since

$$\begin{aligned} & - \log \log 1/F_{x_{T_2}}(x; a, \beta, \nu_{T_2}) \\ &= - \log r - \log \log 1/F_{x_{T_1}}(x; a, \beta, \nu_{T_1}) \end{aligned} \tag{B-6}$$

Comparisons can be easily made by shifting the curve by the amount of $\log r$ when using $-\log \log 1/F(x)$ as the plotting abscissa.

We now come to the problem of estimating the parameters α , β , and ν from a sample X_1, X_2, \dots, X_n . Although there are many methods which may be used to estimate these parameters (e.g., Ref. 2), the method used for this study was that of maximum likelihood (e.g., Ref. 14). The likelihood function is defined as the joint probability density function of the sample:

$$L = \prod_{i=1}^n f(x_i; \alpha, \beta, \nu) = \prod_{i=1}^n \frac{d}{dx} F(x_i, \alpha, \beta, \nu)$$

The maximum likelihood estimates are then the value of the parameters which maximize the likelihood function for the observed sample. Intuitively, this can be visualized as selecting the parameters so as to maximize the probability of occurrence within a small fixed n -dimensional volume about the sample. Maximum likelihood estimates were chosen for several reasons as follows:

(1) They are efficient. That is, the product of sample size and variance of the estimate has the smallest limit as the sample size increases. Other estimates may have the same limiting variance but none will be better.

(2) They are invariant. This is particularly useful when the parameters of interest are not directly estimated. For example, when $\hat{\alpha}$ and $\hat{\beta}$ are maximum likelihood estimates of α and β , invariance means that $\hat{\epsilon} = \hat{\alpha}/\hat{\beta}$ is the maximum likelihood estimate of the limiting distortion, $\epsilon = \alpha/\beta$.

(3) Large sample theory shows that the limiting distribution of the estimates is normal and gives relationships for the limiting variances and covariances. This enables one to compute variance estimates of the estimated parameters, thence to compute approximate confidence intervals for the predicted distortion level as a function of time.

For convenience, the logarithm of the likelihood function is maximized which is equivalent to maximizing the likelihood function since the logarithm is a monotonic increasing function. The required estimates are found by solving the three equations

$$\begin{aligned} \frac{\partial \log L}{\partial \alpha} &\equiv H_1 = 0 \\ \frac{\partial \log L}{\partial \beta} &\equiv H_2 = 0 \\ \frac{\partial \log L}{\partial \nu} &\equiv H_3 = 0 \end{aligned} \tag{B-7}$$

The technique used for this solution is a modified Gauss-Newton iteration based on the method given in Ref. 4. Using a superscript '*' to denote initial guesses for the parameters, Eq. (B-7) are linearized in the form

$$H_j^* + \frac{\partial H_j^*}{\partial a} \Delta a + \frac{\partial H_j^*}{\partial \beta} \Delta \beta + \frac{\partial H_j^*}{\partial \nu} \Delta \nu = 0$$

$$j = 1, 2, 3$$

and then solved for Δa , $\Delta \beta$, and $\Delta \nu$. A quadratic approximation $P(\gamma)$ to ΣH_j^2 is then minimized along the line segment defined by

$$(a^* + \gamma \Delta a, \beta^* + \gamma \Delta \beta, \nu^* + \gamma \Delta \nu)$$

with $0 \leq \gamma \leq 1$ and the quadratic coefficients evaluated utilizing the following three conditions:

$$P(\gamma) = \Sigma H_j^2 \text{ at } \gamma = 0 \text{ and } \gamma = 1$$

$$\frac{dP(\gamma)}{d\gamma} = \frac{d}{d\gamma} \Sigma H_j^2 \text{ at } \gamma = 0$$

Let γ_m denote the value of γ that minimizes $P(\gamma)$ and define

$$H_0 = \text{minimum } \Sigma H_j^2 \quad \gamma_0 = 0, \gamma_m, \text{ or } 1 \\ \gamma = \gamma_0$$

If H_0 occurs at $\gamma_0 = 0$, the quadratic approximation step is repeated over the interval $0 \leq \gamma \leq \gamma_m$ until H_0 occurs at either $\gamma_0 = \gamma_m$ or $\gamma_0 = 1$, in which case the next iteration step is started with parameter guesses of

$$(a^* + \gamma_0 \Delta a, \beta^* + \gamma_0 \Delta \beta, \nu^* + \gamma_0 \Delta \nu)$$

The resulting iterations form a sequence of vectors (a, β, ν) such that the corresponding ΣH_j^2 form a monotonic decreasing sequence. The iterations are repeated until a desired numerical convergence criterion is satisfied.

The asymptotic variance-covariance matrix of these maximum likelihood estimates can be obtained as follows (Ref. 14). Let H_{ij} denote second partial derivatives of $\log L$ with respect to the parameters, for example

$$H_{12} = \frac{\partial^2 \log L}{\partial a \partial \beta}$$

then the expected value of these partials at the maximum likelihood point is approximated by the numerical averages

$$\hat{H}_{ij} = \frac{1}{n} \sum_{k=1}^n H_{ij} (x_k; \hat{a}, \hat{\beta}, \hat{\nu})$$

$$i = 1, 2, 3$$

$$j = 1, 2, 3$$

The variance-covariance matrix is then estimated by

$$[\hat{V}_{ij}] = -\frac{1}{n} [\hat{H}_{ij}]^{-1}$$

An approximation to confidence intervals for the estimated distortion magnitude y as a function of the reduced variate t can be constructed from the variance-covariance matrix elements utilizing a Taylor series. The inverse of Eq. (B-4) can be written

$$y(t) = \frac{a}{\beta} - \left(\frac{a}{\beta} - \nu \right) e^{-\beta t}$$

where

$$t = -\log \log 1/F(y; a, \beta, \nu)$$

thence

$$\begin{aligned} s_y^2 = & \left(\frac{\partial y}{\partial a} \right)^2 \hat{V}_{11} + \left(\frac{\partial y}{\partial \beta} \right)^2 \hat{V}_{22} + \left(\frac{\partial y}{\partial \nu} \right)^2 \hat{V}_{33} \\ & + 2 \frac{\partial y}{\partial a} \frac{\partial y}{\partial \beta} \hat{V}_{12} + 2 \frac{\partial y}{\partial a} \frac{\partial y}{\partial \nu} \hat{V}_{13} + 2 \frac{\partial y}{\partial \beta} \frac{\partial y}{\partial \nu} \hat{V}_{23} \end{aligned} \quad (B-8)$$

By using the return period concept, the estimated cumulative distribution may be used to estimate maximum distortion levels for future intervals. However, the above variance estimates are not the variance of a future observation because the future maximum is a random variable and will contribute an additional source of variation. Denote the future observed maximum by Y and its estimate by \hat{Y} . To obtain a confidence interval for \hat{Y} , the variance of $(Y - \hat{Y})$ is required. Now, Y has an asymptotic distribution given by Eq. (B-4) with the parameters given by Eq. (B-5) where r is the ratio of the time interval of the future maximum to the time interval of the individual extremes of the data sample used to estimate the parameters. The variance of this distribution may be estimated by (Ref. 2)

$$s_Y^2 = \left(\frac{\hat{a}}{\hat{\beta}} - \hat{\nu} \right)^2 [\Gamma(1+2\hat{\beta}) - \Gamma^2(1+\hat{\beta})] \Gamma^{2\hat{\beta}} \quad (\text{B-9})$$

Now \hat{Y} has an asymptotic normal distribution with variance estimate given by Eq. (B-8). Since Y and \hat{Y} are independent, the variance of $Y - \hat{Y}$ is the sum of the two variances and may be estimated by

$$s_{Y-\hat{Y}}^2 = s_Y^2 + s_{\hat{Y}}^2 \quad (\text{B-10})$$

One-sigma limits on Y are then estimated as

$$\hat{Y} - s_{Y-\hat{Y}}, \hat{Y} + s_{Y-\hat{Y}}$$

APPENDIX C

COMPUTER PROGRAM DETAILS

This Appendix provides a brief description of the numerical implementation of the procedure described in Appendix B. The basic data source is presumed available in the form PK_I ; $I = 1, 2, \dots, n$ with optional use of the average and root-mean-square distortion levels as normalizing parameters. Although the authors usually plot the analysis results using Calcomp[®] routines, this coding is not included in the program listing. The program evolved with development of the theoretical approach and could be greatly refined to be more efficient, particularly in the areas of making analytic simplifications of the likelihood function and streamlining the method of solution of the maximum likelihood equations.

DESCRIPTION OF SUBROUTINES

MAIN	Calls CARD and either READB, READC, or READD to obtain basic input data. Calls EVSTAT. Use of external error handling routines is required for the occasional set of bad data or nonconvergence within NLLSQ.
CARD	Calls LISTER. Reads title and option codes from data set 5.
LISTER	Prints input card image.
READB	User-furnished routine for input data source.
READC	Input data from cards, data set 5.
READD	User-furnished routine for input data source on magnetic tape, data set 11.
ORDER	Orders given peaks into ascending magnitude array and generates index of original order.
EVSTAT	Normalize data if desired, calls ORDER. Calls EXTVAL to obtain first and general asymptote solutions. Calls PRNT and/or EVPLOT as desired for output of results.
EXTVAL	Calls NLLSQ for solution of the maximum likelihood equations and VARIAN for computation of the parameter variances.
NLLSQ	General routine for solution of the nonlinear least squares fitting problem using a modified Gauss-Newton iteration. Calls EVAL for computation of partial derivatives and CHOLAS for matrix inversion.

EVAL	Computes partial derivatives of the likelihood function. Note that coding solves for the derivatives with respect to ϵ , $1/\beta$, and ν and then transforms these results to the desired relations. Entry DATSET initializes routine.
CHOLE	General routine for matrix inversion using the method of Cholesky.
VARIAN	Computes parameter variance estimates. Calls EVAL and CHOLE.
PRNT	Prints results on data set 6.
EVPLT	Generates plotted analysis using Calcomp routines. Entry PAGE1 opens and closes plot file.

The following tabulations include a sample input and output using READC and the program listing.

***** CARD INPUT *****

CARD 1111111112222222223333333334444444445555555556666666667777777778
 COLUMN 123456789012345678901234567890123456789012345678901234567890 CARD

SAMPLE CASE OF CARD INPUT DATA --- UN-NORMALIZED

1 1 1 1 0 0
 40 1 14 2 6.1800-01 1.1200-01
 INPUT VAR= 8*0.5,120.1,18,3*0.1,5*0. LEND
 DATA PK1= .931, .765, .757, .970, .880, .839, .851, .933, .891, .772,
 .869, .850, .832, .863, .745, .857, .996, .877, .891, .905,
 .721, .773, .785, .769, .815, .860, .833, .759, .913, .801,
 .820, .829, .838, .766, .794, .915, .788, .911, .881, .903,
 LEND

SAMPLE CASE OF CARD INPUT DATA --- NORMALIZED

1 1 0 1 0 0
 40 1 14 2 6.1800-01 1.1200-01
 INPUT LEND
 DATA LEND

CARD 1111111112222222223333333334444444445555555556666666667777777778
 COLUMN 123456789012345678901234567890123456789012345678901234567890 CARD

EXTREME - VALUE STATISTICS ANALYSIS

PAGE 1

SAMPLE CASE OF CARD INPUT DATA --- UN-NORMALIZED

IO = 0. PART 0. POINT 0.

SEGMENT START TIME 0. 0. 0. 0. 0. NUMBER OF EXTREMES 40

SEQUENCE 0.

RANK	ORDER	DATA	NORMDATA	NORMVAR	T	RANK	ORDER	DATA	NORMDATA	NORMVAR	T
1	37	0.9310	0.9310	0.7210	-1.3120	21	1	0.7210	0.7210	0.8500	0.4019
2	5	0.7650	0.7650	0.7450	-1.1054	22	9	0.7730	0.7730	0.8510	0.4740
3	3	0.7570	0.7570	0.7570	-0.9612	23	10	0.7850	0.7850	0.8570	0.5480
4	39	0.9700	0.9700	0.7590	-0.8447	24	7	0.7690	0.7690	0.8600	0.6245
5	28	0.8800	0.8800	0.7650	-0.7439	25	14	0.8150	0.8150	0.8630	0.7038
6	20	0.8390	0.8390	0.7660	-0.6533	26	24	0.8600	0.8600	0.8690	0.7864
7	22	0.8510	0.8510	0.7690	-0.5697	27	18	0.8330	0.8330	0.8770	0.8729
8	38	0.9330	0.9330	0.7720	-0.4911	28	4	0.7590	0.7590	0.8800	0.9640
9	31	0.8910	0.8910	0.7730	-0.4163	29	35	0.9130	0.9130	0.8810	1.0605
10	8	0.7720	0.7720	0.7850	-0.3443	30	13	0.8010	0.8010	0.8910	1.1636
11	26	0.8690	0.8690	0.7880	-0.2744	31	15	0.8200	0.8200	0.8910	1.2745
12	21	0.8500	0.8500	0.7940	-0.2059	32	16	0.8290	0.8290	0.9030	1.3950
13	17	0.8320	0.8320	0.8010	-0.1386	33	19	0.8380	0.8380	0.9050	1.5276
14	25	0.8630	0.8630	0.8150	-0.0719	34	6	0.7660	0.7660	0.9110	1.6755
15	2	0.7450	0.7450	0.8200	-0.0055	35	12	0.7940	0.7940	0.9130	1.8437
16	23	0.8570	0.8570	0.8290	0.0608	36	36	0.9150	0.9150	0.9150	2.0394
17	40	0.9960	0.9960	0.8320	0.1274	37	11	0.7880	0.7880	0.9310	2.2764
18	27	0.8770	0.8770	0.8330	0.1946	38	34	0.9110	0.9110	0.9330	2.5772
19	30	0.8910	0.8910	0.8380	0.2625	39	29	0.8810	0.8810	0.9700	2.9955
20	33	0.9050	0.9050	0.8390	0.3315	40	32	0.9030	0.9030	0.9960	3.7013

EXTREME-VALUE STATISTICS ANALYSIS

PAGE 2

SAMPLE CASE OF CARO INPUT DATA --- UN-NORMALIZED

IO = 0. PART 0. POINT 0.

SEGMENT START TIME 0. 0. 0. 0. 0. NUMBER OF EXTREMES 40

SEQUENCE 0.

OPTION CODES 1 1 1 1 0 0 0 0 0 0

AVG = 0.6180 RMS = 0.1120

MAXIMUM LIKELIHOOD ESTIMATES: FIRST ASYMPTOTE

THIRD ASYMPTOTE

CORRELATION COEFFICIENTS

MODAL PARAMETER 0.8120 * 0.0097
SLOPE PARAMETER 17.2736 * 2.0922
MOMENT
LIMIT ESTIMATE

0.8192 * 0.0110
0.2453 * 0.1041
0.2242 * 0.1200
1.0938 * 0.4642

1-2 0.42689
1-3 0.41493
2-3 0.99796

VARIANCE-COVARIANCE MATRICES 0.938790-04
-0.664650-02

-0.664650-02
0.437730 01

0.120350-03
0.487500-03
0.546400-03

0.487500-03 0.546400-03
0.108360-01 0.124700-01
0.124700-01 0.144080-01

CONVERGENCE CODE, NO. OF ITERATIONS

0. 4. 0. 17.

EVALUATION OF MAXIMUM LIKELIHOOD ESTIMATE RESULTS

T	FIRST ASYMPTOTE			THIRD ASYMPTOTE			RETURN PERIOD, SEC
	VALUE	MIN	MAX	VALUE	MIN	MAX	
-2.00	0.6963	0.6821	0.7104	0.6638	0.6496	0.6780	2.001E-01
-1.50	0.7252	0.7135	0.7369	0.7094	0.6977	0.7211	2.023E-01
-1.00	0.7541	0.7442	0.7641	0.7502	0.7402	0.7601	2.141E-01
-0.50	0.7831	0.7739	0.7922	0.7866	0.7775	0.7958	2.476E-01
0.0	0.8120	0.8023	0.8217	0.8192	0.8095	0.8289	3.164E-01
0.50	0.8410	0.8296	0.8523	0.8483	0.8370	0.8597	4.398E-01
1.00	0.8699	0.8562	0.8836	0.8744	0.8607	0.8880	6.498E-01
1.50	0.8989	0.8824	0.9153	0.8976	0.8812	0.9141	1.000E 00
2.00	0.9278	0.9083	0.9473	0.9184	0.8989	0.9379	1.580E 00
2.50	0.9568	0.9341	0.9794	0.9370	0.9144	0.9597	2.538E 00
3.00	0.9857	0.9598	1.0116	0.9537	0.9278	0.9795	4.118E 00
3.50	1.0147	0.9855	1.0438	0.9685	0.9393	0.9977	6.724E 00
4.00	1.0436	1.0111	1.0761	0.9818	0.9493	1.0143	1.102E 01
4.50	1.0725	1.0366	1.1085	0.9937	0.9578	1.0296	1.810E 01
5.00	1.1015	1.0622	1.1408	1.0043	0.9650	1.0436	2.978E 01
5.50	1.1304	1.0877	1.1732	1.0138	0.9711	1.0565	4.904E 01
6.00	1.1594	1.1132	1.2056	1.0223	0.9761	1.0684	8.079E 01
6.50	1.1883	1.1387	1.2379	1.0299	0.9803	1.0795	1.331E 02
7.00	1.2173	1.1642	1.2703	1.0366	0.9836	1.0897	2.194E 02
7.50	1.2462	1.1897	1.3027	1.0427	0.9862	1.0992	3.617E 02
8.00	1.2752	1.2152	1.3351	1.0481	0.9882	1.1081	5.963E 02
8.40	1.1823	1.1334	1.2312	1.0284	0.9795	1.0773	1.200E 02

OBSERVED PEAK 1.1800 IN 120.0 SEC

ESTIMATES BASED ON DATA FROM 8.0 SEC

STATISTICS = -0.05 3.17

EXTREME-VALUE STATISTICS ANALYSIS

PAGE 3

SAMPLE CASE OF CARD INPUT DATA --- NORMALIZED

ID # 1. PART 14. POINT 2.

SEGMENT START TIME 0. 0. 0. 0. 0. NUMBER OF EXTREMES 40

SEQUENCE 2.

RANK	ORDER	DATA	NORMDATA	NORMVAR	T	RANK	ORDER	DATA	NORMDATA	NORMVAR	T
1	37	0.9310	2.7946	0.9196	-1.3120	21	1	0.7210	0.9196	2.0714	0.4019
2	5	0.7650	1.3125	1.1339	-1.1054	22	9	0.7730	1.3839	2.0804	0.4740
3	3	0.7570	1.2411	1.2411	-0.9612	23	10	0.7850	1.4911	2.1339	0.5480
4	39	0.9700	3.1429	1.2589	-0.8447	24	7	0.7690	1.3482	2.1607	0.6245
5	28	0.8800	2.3393	1.3125	-0.7439	25	14	0.8150	1.7589	2.1875	0.7038
6	20	0.8390	1.9732	1.3214	-0.6533	26	24	0.8600	2.1607	2.2411	0.7864
7	22	0.8510	2.0804	1.3482	-0.5697	27	18	0.8330	1.9196	2.3125	0.8729
8	38	0.9330	2.8125	1.3750	-0.4911	28	4	0.7590	1.2589	2.3393	0.9640
9	31	0.8910	2.4375	1.3839	-0.4163	29	35	0.9130	2.6339	2.3482	1.0605
10	8	0.7720	1.3750	1.4911	-0.3443	30	13	0.8010	1.6339	2.4375	1.1636
11	26	0.8690	2.2411	1.5179	-0.2744	31	15	0.8200	1.8036	2.4375	1.2745
12	21	0.8500	2.0714	1.5714	-0.2059	32	16	0.8290	1.8839	2.5446	1.3950
13	17	0.8320	1.9107	1.6339	-0.1386	33	19	0.8380	1.9643	2.5625	1.5276
14	25	0.8630	2.1875	1.7589	-0.0719	34	6	0.7660	1.3214	2.6161	1.6755
15	2	0.7450	1.1339	1.8036	-0.0055	35	12	0.7940	1.5714	2.6339	1.8437
16	23	0.8570	2.1339	1.8839	0.0608	36	36	0.9150	2.6518	2.6518	2.0398
17	40	0.9960	3.3750	1.9107	0.1274	37	11	0.7880	1.5179	2.7946	2.2764
18	27	0.8770	2.3125	1.9196	0.1946	38	34	0.9110	2.6161	2.8125	2.5772
19	30	0.8910	2.4375	1.9643	0.2625	39	29	0.8810	2.3482	3.1429	2.9955
20	33	0.9050	2.5625	1.9732	0.3315	40	32	0.9030	2.5446	3.3750	3.7013

EXTREME-VALUE STATISTICS ANALYSIS

PAGE 4

SAMPLE CASE OF CARD INPUT DATA --- NORMALIZED

IO = 1. PART 14. POINT 2.

SEGMENT START TIME 0. 0. 0. 0. 0.

NUMBER OF EXTREMES 40

SEQUENCE 2.

OPTION CODES 1 1 0 1 0 0 0 0 0 0

AVG = 0.6180 RMS = 0.1120

MAXIMUM LIKELIHOOD ESTIMATES: FIRST ASYMPTOTE

THIRD ASYMPTOTE

CORRELATION COEFFICIENTS

MODAL PARAMETER 1.7325 * 0.0865
SLOPE PARAMETER 1.9346 * 0.2343
MOMENT
LIMIT ESTIMATE

1.7964 * 0.0980
0.9526 * 0.2718
0.2242 * 0.1200
4.2482 * 1.2119

1-2 0.44870
1-3 0.41493
2-3 0.97591

VARIANCE-COVARIANCE MATRICES 0.748400-02
-0.664650-02

-0.664650-02
0.549090-01

0.959440-02
0.119440-01
0.487850-02

0.119440-01 0.487850-02
0.738500-01 0.318340-01
0.318340-01 0.144080-01

CONVERGENCE CODE, NO. OF ITERATIONS 0 3 0 12

EVALUATION OF MAXIMUM LIKELIHOOD ESTIMATE RESULTS

T	FIRST ASYMPTOTE			THIRD ASYMPTOTE			RETURN PERIOD, SEC
	VALUE	MIN	MAX	VALUE	MIN	MAX	
-2.00	0.6987	0.5720	0.8254	0.4089	0.2821	0.5356	2.001E-01
-1.50	0.9571	0.8524	1.0619	0.8161	0.7113	0.9208	2.023E-01
-1.00	1.2156	1.1270	1.3042	1.1801	1.0915	1.2687	2.141E-01
-0.50	1.4740	1.3922	1.5558	1.5055	1.4237	1.5872	2.476E-01
0.0	1.7325	1.6460	1.8190	1.7964	1.7098	1.8829	3.164E-01
0.50	1.9909	1.8897	2.0921	2.0564	1.9552	2.1576	4.398E-01
1.00	2.2494	2.1271	2.3716	2.2889	2.1666	2.4112	6.498E-01
1.50	2.5078	2.3607	2.6549	2.4967	2.3496	2.6437	1.000E 00
2.00	2.7662	2.5923	2.9402	2.6824	2.5085	2.8564	1.580E 00
2.50	3.0247	2.8226	3.2268	2.8485	2.6464	3.0506	2.538E 00
3.00	3.2831	3.0520	3.5143	2.9970	2.7658	3.2281	4.118E 00
3.50	3.5416	3.2810	3.8022	3.1297	2.8690	3.3903	6.724E 00
4.00	3.8000	3.5095	4.0906	3.2483	2.9578	3.5388	1.102E 01
4.50	4.0585	3.7378	4.3792	3.3543	3.0337	3.6750	1.810E 01
5.00	4.3169	3.9659	4.6680	3.4491	3.0981	3.8062	2.978E 01
5.50	4.5754	4.1938	4.9569	3.5339	3.1523	3.9155	4.904E 01
6.00	4.8338	4.4216	5.2460	3.6097	3.1975	4.0218	8.079E 01
6.50	5.0923	4.6494	5.5352	3.6774	3.2345	4.1263	1.331E 02
7.00	5.3507	4.8770	5.8244	3.7379	3.2642	4.2116	2.194E 02
7.50	5.6092	5.1046	6.1137	3.7920	3.2875	4.2966	3.617E 02
8.00	5.8676	5.3321	6.4031	3.8404	3.3049	4.3759	5.963E 02
6.40	5.0387	4.6022	5.4753	3.6640	3.2274	4.1005	1.200E 02

OBSERVED PEAK 5.0179 IN 120.0 SEC

ESTIMATES BASED ON DATA FROM 8.0 SEC

STATISTICS = -0.05 3.17

```

C      EXTREME-VALUE STATISTICS ANALYSIS
C
C      IOPT(1) POINTS TO DATA SOURCE
C          = 1  CARD INPUT
C          = 2  DISK FILE
C          = 3  TAPE
C      IOPT(2) SPECIFIES PRINT 1, PLOT 2, BOTH 0
C      IOPT(3)=0 FOR NORMALIZATION BY AVG,RMS      =1 FOR NO ADJUSTMENT
C      IOPT(4)= NUMBER OF SOLUTIONS PER INPUT SET
C      IOPT(5) = SPECIFIED NPK IF NOT = 0
C      IOPT(6) = PLOT SCALE SPECIFICATION
C          = 0 DEFAULT SCALES
C          = 1 COMPUTE SCALES
C          VAR(1)=ID
C          VAR(11) = PEAK
C          2 =PART
C          12 = VMIN PLOT SCALE
C          3 =POINT
C          13 = YMAX PLOT SCALE
C          4 =START TIME,DAY
C          14 = YINC PLOT SCALE
C          5 =HOUR
C          15 = SIGMA LEVEL
C          6 =MIN
C          16 =
C          7 =SEC
C          17 =
C          8 =MSEC
C          18 =
C          9 =SAMPLE RATE PER SEC
C          19 =
C          10 =PEAK TIME (SEC)
C          20 = SEQUENCE
C
C      DIMENSION PK(300)
C      COMMON /TITLE/ TIT(20),VAR(20)
C      COMMON /OPTION/ IOPT(10)
C      CALL ERRSET(207,256,-1,1)
C      CALL ERRSET(208,256,-1,1)
C      CALL ERRSET(209,256,-1,1)
C      CALL ERRSET(252,256,-1,1)
C      CALL ERRSET(253,256,-1,1)
C      CALL ERRSET(261,256,-1,1)
C      CALL ERRSET(263,256,-1,1)
10 CALL CARD
20 CONTINUE
  IF(IOPT(1).EQ.1) CALL READC(N,AVG,RMS,PK)
  IF(IOPT(1).EQ.2) CALL READB(N,AVG,RMS,PK)
  IF(IOPT(1).EQ.3) CALL READD(N,AVG,RMS,PK)
  CALL EVSTAT(N,AVG,RMS,PK)
  IOPT(4)=IOPT(4)-1
  IF(IOPT(4).GT.0) GO TO 20
  IF(IOPT(1).EQ.3) REWIND 11
  GO TO 10
END

```

```

      SUBROUTINE CARD
      COMMON /TITLE/ TIT(20),VAR(20)
      COMMON /OPTION/ IOPT(10)
      DATA ID/0/,N/5/
      DATA IPLOT/0/
      IF(ID.EQ.0) CALL LISTER(6)
      ID=ID+1
      READ(N,1,END=100) TIT,IOPT
1    FORMAT(20A4 /10I5)
      VAR(20)=ID
      IF%IOPT%2<.NE.1 .AND. IPLOT.EQ.0< IPLOT#1
      RETURN
C      CLOSE EVPLOT FROM CARD END
100 IF%IPLOT.EQ.0< STOP
      CALL PAGE1(8)
      END

```

```

      SUBROUTINE LISTER(K)
      REAL*4 C(20)
      DATA KARD/1/
      REWIND 5
10  WRITE(K,11)
11  FORMAT(1H1,4(/),1X,43(1H*),12H CARD INPUT ,43(1H*))
      WRITE(K,12)
12  FORMAT(/,5H CARD,T20,10(1H1),10(1H2),10(1H3),10(1H4),10(1H5),10(1H
*6),10(1H7),1H8,/,7H COLUMN,T11,8(10H1234567890),5X,4HCARD,/)
      DO 30 J=1,45
20  READ(5,21,END=40) C
21  FORMAT(20A4)
      WRITE(K,22) C,KARD
22  FORMAT(10X,20A4,I8)
      KARD=KARD+1
30  CONTINUE
      WRITE(K,12)
      GO TO 10
40  REWIND 5
      WRITE(K,12)
      RETURN
      END

```

```

SUBROUTINE READC(N,AVG,RMS,PK)
  DIMENSION PK(300)
  DIMENSION PKI(300)
  COMMON /TITLE/ TIT(20),VAR(20)
  COMMON /OPTION/ IOPT(10)
  NAMELIST /INPUT/ VAR /DATA/ PKI
  READ(5,1) N,ID,NPRT,NPT,AVG,RMS
1  FORMAT(4I5,2E10.4)
  VAR(15)=1.
  VAR(1)=ID
  VAR(2)=NPRT
  VAR(3)=NPT
  READ(5,INPUT)
  READ(5,DATA)
  DO 10 I=1,N
    PK(I)=PKI(I)
10 CONTINUE
  IF (IOPT(3).EQ.0) VAR(11)=(VAR(11)-AVG)/RMS
  RETURN
  END

```

```

SUBROUTINE ORDER(T)
  REAL*8 X
  DIMENSION T(300)
  COMMON /EVALX/ X(300),NPK
  COMMON /ORD/ K(300)
  N=NPK
  TMIN=1.D50
  DO 10 I=1,N
10  K(I)=0
    DO 30 I=1,N
      DO 20 J=1,N
        IF(K(J)) 20,11,20
11  IF(T(J)-TMIN) 12,12,20
12  KK=J
        TMIN=T(J)
20  CONTINUE
        K(KK)=I
        TMIN=1.D50
30  CONTINUE
    DO 40 I=1,N
      X(K(I))=DBLE(T(I))
40  CONTINUE
  RETURN
  END

```



```

C
C
C
C
C
SUBROUTINE EVSTAT (N , AVG, RMS, PK )

      N = NO. OF PEAKS
      AVG = TIME AVERAGED DISTORTION
      RMS = ROOT-MEAN-SQUARE OF DISTORTION
      PK = UNORDERED ARRAY OF DISTORTION PEAKS

      REAL*8 X,S1,S3,V1,V3
      DIMENSION PK(N),T(300),S1(10),S3(10),V1(3,6),V3(3,6)
      COMMON /EVALX/ X(300),NPK
      COMMON /TITLE/ TIT(20),VAR(20)
      COMMON /OPTION/ IOPT(10)
      NPK=N
      IF(IOPT(3)) 20,10,20
10 DO 15 I=1,N
15 T(I)=(PK(I)-AVG)/RMS
      GO TO 30
20 DO 25 I=1,N
25 T(I)=PK(I)
30 CONTINUE
      CALL ORDER(T)
      S1(1)=X(NPK/3)
      S1(2)=(-ALOG(ALOG((1.+NPK)/NPK)))+ALOG(ALOG(1.+NPK)))/(X(NPK)-X(1))
      CALL EXTVAL(2,S1,V1)
      S3(1)=S1(1)
      S3(4)=2.*X(NPK)
      S3(3)=1.D0/(S1(2)*(S3(4)-S3(1)))
      S3(2)=S3(3)*S3(4)
      CALL EXTVAL(3,S3,V3)
      VAR(16)=V3(1,5)/DSQRT(V3(1,4)*V3(2,5))
      VAR(17)=V3(1,6)/DSQRT(V3(1,4)*V3(3,6))
      VAR(18)=V3(2,6)/DSQRT(V3(2,5)*V3(3,6))
      IF(IOPT(2).EQ.2) GO TO 40
      CALL PRNT(S1,S3,V1,V3,AVG,RMS,PK,T)
40 IF(IOPT(2).EQ.1) GO TO 50
      IF%IOPT%6<.EQ.1< CALL SCALE
      CALL EVPLOT(S1,S3,AVG,RMS,V1,V3)
50 CONTINUE
      RETURN
      END

SUBROUTINE EXTVAL(KODE,S,V)
      REAL*8 S,V,Y,X
      DIMENSION S(10),V(3,6),Y(300)
      COMMON /EVALX/ X(300),NPK
      DO 10 I=1,NPK
10 Y(I)=0.
      CALL NLLSQ(KODE,S,Y)
      CALL VARIAN(KODE,S,V)
      RETURN
      END

```

```

SUBROUTINE NLLSQ(KODE,GUESS,Y)
IMPLICIT REAL*8 (A-H,O-Z)
DIMENSION X(300),Y(300),GUESS(10),THETA(10),Q(10),D(10),FMAT(10,10
*)
DATA IT/200/,TOL/1D-8/,ATOL/1D-10/,ISW2/0/,ISW3/0/
DATA KSYM/0/
C      ROUTINE NORMALLY FITS Y=F(X), X USED NOW AS POINTER ONLY, Y=0
C      NP NORMALLY NO. OF PARAMETERS      NS NO. OF SAMPLES
GUESS(10)=0.
C      GUESS(10) = CONVERGENCE CODE
C                  = 0 OK      =1 MAXIMUM IT      =2 POSITIVE DERIVATIVE
C                  =3 TOO MANY CUTBACKS
NOBS=KODE
NP=KODE
ICLK=0
ITG=0
DO 1 I=1,KODE
1 X(I)=I
NQ=0
II=0
NS=KODE
CALL DATSET(GUESS,KODE)
QZERO=0.0
DO 5 I=1,10
5 THETA(I)=GUESS(I)
10 CONTINUE
100 CONTINUE
ITN=1
DO 110 I=1,NS
XX=X(I)
F=EVAL(XX,GUESS,NP,0)
110 QZERO=QZERO+Y*I<-F<=.2
120 QHALF=0.0
KOUNT=0
QONE=0.0
QVMIN=0.0
DO 130 J=1,NP
D(J)=0.0
Q(J)=0.0
DO 130 K=1,NP
130 FMAT(J,K)=0.0
DO 150 I=1,NP
DO 150 J=I,NP
DO 140 K=1,NS
XX=X(K)
140 FMAT(I,J)=FMAT(I,J)+EVAL(XX,GUESS,NP,I)*EVAL(XX,GUESS,NP,J)
150 FMAT(J,I)=FMAT(I,J)
DO 170 J=1,NP
DO 160 I=1,NS
XX=X(I)
F=EVAL(XX,GUESS,NP,0)
Q(J)=Q(J)+(Y(I)-F)*EVAL(XX,GUESS,NP,J)
160 CONTINUE

```

```

170 CONTINUE
    DO 210 J=1,NP
210  FMAT(J,NP+1)=Q(J)
        ID2=4
        ID2=5
        CALL CHOLES(FMAT,NP,1,10,ID2,2)
        DO 200 J=1,NP
200  O(J)=FMAT(J,NP+1)
        DERIV = 0.0
        DO 221 J=1,NP
221  DERIV = DERIV-D(J)*Q(J)
        IF (DERIV .GE. 0.0) GO TO 222
        DO 230 I=1,NP
230  THETA(I)=GUESS(I)+O(I)
        DO 240 I=1,NS
            XX=X(I)
            F=EVAL(XX,THETA,NP,0)
240  QONE=QONE + (Y(I)-F)**2
227 CONTINUE
            QVMIN=0.0
            DENOM=QONE-QZERO-DERIV
            IF (DENOM .LE. 0.0) GO TO 223
            VMIN = -0.5*DERIV/DENOM
            IF (VMIN.GE.1.0) GO TO 223
            IF (VMIN.LT.0.1) VMIN=0.1
            DO 270 I=1,NP
270  THETA(I) = GUESS(I)+VMIN*O(I)
            DO 280 I=1,NS
                XX=X(I)
                F=EVAL(XX,THETA,NP,0)
                QVMIN=QVMIN+(Y(I)-F)**2
280 CONTINUE
            IF (QVMIN .GT. QZERO+ATOL) GO TO 225
224 CONTINUE
            DO 290 I=1,NP
290  GUESS(I)=GUESS(I)+VMIN*O(I)
            IF (QVMIN.LT.ATOL) GO TO 330
            IF (DABS((QVMIN-QZERO)/QVMIN).LE.TOL) GO TO 1111
300 IF (ITN=IT) 320,310,310
310 CONTINUE
            GUESS(10)=100
            L=L+1
            GO TO 330
320 QZERO=QVMIN
            ITN=ITN+1
            GO TO 120
1111 CONTINUE
330 IF (ISW3=1) 370,340,370
340 IF (II) 370,350,370
350 NS=NOBS
            II=1
            ITN=1
            GO TO 120
370 CONTINUE

```

```

      IF(KOUNT.GT.5) GUESS(10)=300
      GUESS(9)=ITN
      IF(KODE.EQ.2) RETURN
      IF(KODE.EQ.3) RETURN
      GO TO 1
600  CONTINUE
222  CONTINUE
      GUESS(10)=200
      RETURN
223  VMIN = 1.0
      QVMIN = QONE
      GO TO 224
225  IF (QONE .LT. QZERO) GO TO 223
      KOUNT=KOUNT+1
      DO 226 J=1,NP
226  D(J) = VMIN*D(J)
      QONE = QVMIN
      DERIV=DERIV*VMIN
      GO TO 227
      END

```

```

      FUNCTION EVAL(X,C,N,K)
      IMPLICIT REAL*8 (A-H,O-Z)
      DIMENSION C%10<
      COMMON /EVALX/ Y(300),NPK
      IF(KODE.EQ.3) GO TO 100
      IF(V.NE.C(1))GO TO 10
      IF(A.NE.C(2))GO TO 10
      GO TO 20
10  CONTINUE
      V=C(1)
      A=C(2)
      S0=NPK
      S1=0.
      S2=0.
      S3=0.
      S4=0.
      S5=0.
      DO 15 I=1,NPK
      E=Y(I)-V
      PHI=DEXP(-A*E)
      S1=S1+1.D0-PHI
      S2=S2+E*(1.D0-PHI)
      S3=S3+PHI
      S4=S4+PHI*E
      S5=S5+PHI*E**2
15  CONTINUE
      T1=A*S1
      T2=S0/A -S2
      T11=-S3*A**2
      T12=S1+A*S4
      T22=-S0/A**2-S5
20  KK=X

```

```

      GO TO (30,40),K
      GO TO (21,22),KK
21  EVAL=T1
      RETURN
22  EVAL=T2
      RETURN
30  GO TO (31,32),KK
31  EVAL=T11
      RETURN
32  EVAL=T12
      RETURN
40  GO TO (32,42),KK
42  EVAL=T22
      RETURN
100 CONTINUE
      IF(V.NE.C(1)) GO TO 110
      IF(A.NE.C(2)) GO TO 110
      IF(B.NE.C(3)) GO TO 110
      GO TO 120
110 CONTINUE
      V=C(1)
      E=C(2)
      A=C(2)
      B=C(3)
      XK=1/B
      E=A*XK
      S0=NPK
      S1=0.
      S2=0.
      S3=0.
      S4=0.
      S5=0.
      S6=0.
      S7=0.
      S8=0.
      S9=0.
      S10=0.
      DO 115 I=1,NPK
      PHI=(E-Y(I))/(E-V)
      PHIK=PHI**XK
      PHIL=DLOG(PHI)
      S1=S1+PHIK
      S2=S2+1D0/PHI
      S3=S3+PHIK*PHI
      S4=S4+PHIL
      S5=S5+PHIK*PHIL
      S6=S6+PHIK/PHI
      S7=S7+1D0/PHI**2
      S8=S8+PHIK/PHI**2
      S9=S9+PHIL*PHIK/PHI
      S10=S10+PHIK*PHIL**2
115 CONTINUE

```

```

EV=E-V
T1=(S0-S1)*XK/EV
T2=(-XK*S0+(XK-1)*S2+XK*S1-XK*S6)/EV
T3=S0/XK+S4-S5
T11=(S0-(XK+1)*S1)*XK/EV**2
T12=(-S0-XK*S6+(XK+1)*S1)*XK/EV**2
T13=(S0-S1-XK*S5)/EV
T22=(S0-(XK-1)/XK*S7+XK*2*S6-(XK+1)*S1-(XK-1)*S8)*XK/EV**2
T23=(-S0+S2-XK*S9+XK*S5-S6+S1)/EV
T33=(-S0*XK**2-XK**4*S10)
T33=T33+XK**3*2*T3
T33=T33 + E**2*XK**2*T22 + 2.*E*XK**2*T2 + 2.*E*XK**3*T23
T23 = - XK**3*T23 - E*XK**2*T22 - XK**2*T2
T22= XK**2*T22
T3=-T3*XK**2
T3=T3 - E*XK*T2
T2=XK*T2
T13 = - XK**2*T13 - E*XK*T12
T12 = XK*T12
120 KK=X
GO TO(130,140,150),K
GO TO(121,122,123),KK
121 EVAL=T1
RETURN
122 EVAL=T2
RETURN
123 EVAL=T3
RETURN
130 GO TO(131,132,133),KK
131 EVAL=T11
RETURN
132 EVAL=T12
RETURN
133 EVAL=T13
RETURN
140 GO TO(132,142,143),KK
142 EVAL=T22
RETURN
143 EVAL=T23
RETURN
150 GO TO (133,143,153),KK
153 EVAL=T33
RETURN
ENTRY DATSET(C,KODE)
DATSET=0
RETURN
END

```

```

SUBROUTINE CHOLAS(A,N,NV,ID1,ID2,MATSYM)
REAL*8 A(ID1,ID2),SUM,TEMP
CUT=0.
M=N+NV
NARD=N+1
IF(A(1,1).NE.0.0) GO TO 47
DO 37 J=2,N
IF(A(J,1).EQ.0.0) GO TO 37
IFLIP=J
GO TO 27
37 CONTINUE
GO TO 54321
27 DO 57 K=1,M
TEMP=A(IFLIP,K)
A(IFLIP,K)=A(1,K)
A(1,K)=TEMP
57 CONTINUE
47 DO 2 J=2,M
A(1,J)=A(1,J)/A(1,1)
2 CONTINUE
DO 6 I=2,N
DO 7 J=2,M
IF(MATSYM.EQ.0)GO TO 49
IF(I-J)69,68,67
49 IF(J.GT.I)GO TO 69
68 K=J-1
SUM=0.0
DO 3 IR=1,K
SUM=SUM+A(I,IR)*A(IR,J)
3 CONTINUE
D=A(I,J)
A(I,J)=A(I,J)-SUM
IF (MATSYM.NE.2) GO TO 7
D=A(I,J)/D
101 FORMAT('SINGULAR MATRIX, I = ',I2)
IF (D.GT.CUT) GO TO 7
DO 88 KRK=1,N
88 A(KRK,J) =0.0
DO 89 KRK=1,M
89 A(J,KRK) =0.0
A(J,J)=-ABS(D)
GO TO 7
69 K=I-1
SUM=0.0
DO 4 IR=1,K
SUM=SUM+A(I,IR)*A(IR,J)
4 CONTINUE
IF(A(I,I).EQ.0.0) GO TO 54321
A(I,J)=(A(I,J)-SUM)/A(I,I)
GO TO 7
67 A(I,J)=A(J,I)*A(J,J)
7 CONTINUE

```

```

6  CONTINUE
   DO 52 NPROB=NARD,M
   DO 52 K=2,N
   I=N+1-K
   SUM=0.0
   LL=I+1
   DO 51 IR=LL,N
   SUM=SUM+A(I,IR)*A(IR,NPROB)
51  CONTINUE
   A(I,NPROB)=A(I,NPROB)-SUM
52  CONTINUE
   GO TO 12345
54321 N=-1
12345 RETURN
      END

      SUBROUTINE VARIAN(KODE,S,V)
      IMPLICIT REAL*8 (A-H,O-Z)
      DIMENSION S(10),V(3,6),A(3,6),AS(3,6)
      TOL=1.00
      N=KODE
      M=2*N
      DO 40 I=1,N
      K=I+N
      X=I
      DO 30 J=1,N
      A(I,J)=-EVAL(X,S,N,J)
30  A(J,K)=0.
40  A(I,K)=1.00
      DO 50 I=1,N
      DO 50 J=1,M
50  AS(I,J)=A(I,J)
      CALL CHOLES(A,N,N,3,5,2)
      DO 60 I=1,N
      DO 60 J=1,M
60  V(I,J)=A(I,J)
      DO 70 I=1,N
      J=I+4
      K=I+N
70  S(J)=TOL*DSQRT(V(I,K))
      IF(KODE.EQ.2) RETURN
C      SOLVE FOR LIMIT VARIANCE FOR KODE=3
      EP=S(3)/S(2)
      AS(2,2)=S(3)**2*(AS(2,2)-2.*EP*AS(2,3)+EP**2*AS(3,3))
      AS(2,3)=S(3)*(AS(2,3)-EP*AS(3,3))
      AS(1,2)=S(3)*(AS(1,2)-EP*AS(1,3))
      AS(2,1)=AS(1,2)
      AS(3,2)=AS(2,3)
      DO 90 I=1,N
      K=I+N
      DO 80 J=1,N
80  AS(J,K)=0.
90  AS(I,K)=1.00
      CALL CHOLES(AS,N,N,3,5,2)
      S(4)=S(2)/S(3)
      S(8)=TOL*DSQRT(AS(2,5))
      RETURN
      END

```



```

SUBROUTINE PRNT(S1,S3,V1,V3,AVG,RMS,PK,T)
REAL*8 S1,S3,V1,V3,X
DIMENSION S1(10),S3(10), V1(3,6), V3(3,6), PK(300), T(300)
COMMON /EVALX/ X(300),NPK
COMMON /TITLE/ TIT(20),VAR(20)
COMMON /OPTION/ IOPT(10)
COMMON /ORD / KORD(300)
COMMON /MISC/ RP(300),TP(300)
DATA NPAG/0/,NLIN/0/,N/6/
NPK2=NPK/2
NLIN=0
1 FORMAT(1H1,20X,'E X T R E M E - V A L U E   S T A T I S T I C S
  *A N A L Y S I S',T122,'PAGE ',I3,/,1H0,20A4,10X,'ID'=',F6.0,5X,
  *'PART',F6.0,5X,'POINT',F4.0,/)
2 FORMAT(1H , 'SEGMENT START TIME ',F4.0,3F3.0,F4.0,T118,'SEQUENCE ',
  *F4.0,T49,'NUMBER OF EXTREMES',I4,/)
DO 10 I=1,NPK
  TP(I)=-ALOG(ALOG((1.+NPK)/FLOAT(I)))
10 CONTINUE
  LPP=50
15 DO 30 I=1,NPK2
  IF(NLIN/LPP*.LPP.NE.NLIN) GO TO 20
  NPAG=NPAG+1
  WRITE(N,1) NPAG,TIT,(VAR(K),K=1,3)
  WRITE(N,2) (VAR(K),K=4,8),VAR(20),NPK
  WRITE(N,16)
16 FORMAT(1H0,'RANK ORDER DATA NORMDATA NORMVAR T',
  * T61,'RANK ORDER DATA NORMDATA NORMVAR T',/)
17 FORMAT(1H ,I3,I7,4F9.4,T61,I3,I7,4F9.4)
20 CONTINUE
  NLIN=NLIN+1
  J=I+NPK/2
  WRITE(N,17) I,KORD(I),PK(I),T(I),X(I),TP(I),J,KORD(J),PK(J),T(J),
  *X(J),TP(J)
30 CONTINUE
  NPAG=NPAG+1
  WRITE(N,1) NPAG,TIT,(VAR(I),I=1,3)
  WRITE(N,2) (VAR(I),I=4,8),VAR(20),NPK
  WRITE(N,31) IOPT,AVG,RMS
31 FORMAT(10 OPTION CODES ',10I5,26X,'AVG =',F9.4,5X,'RMS =',F9.4,/)
  WRITE(N,32)
32 FORMAT(10MAXIMUM LIKELIHOOD ESTIMATES: FIRST ASYMPTOTE',T62,
  *'THIRD ASYMPTOTE',T90,'CORRELATION COEFFICIENTS',/)
  WRITE(N,33) S1(1),S1(5),S3(1),S3(5),VAR(16)
33 FORMAT(1H ,5X,'MODAL PARAMETER',T30,F7.4,' * ',F7.4,T60,F7.4,' * '
  *',F7.4,T95,'1-2',5X,F8.5)
  WRITE(N,34) S1(2),S1(6),S3(2),S3(6),VAR(17)
34 FORMAT(1H ,5X,'SLOPE PARAMETER',T30,F7.4,' * ',F7.4,T60,F7.4,' * '
  *',F7.4,T95,'1-3',5X,F8.5)
  WRITE(N,35) S3(3),S3(7),VAR(18)
35 FORMAT(1H ,5X,'MOMENT',T60,F7.4,' * ',F7.4,T95,'2-3',5X,F8.5)
  WRITE(N,36) S3(4),S3(8)
36 FORMAT(1H ,5X,'LIMIT ESTIMATE',T59,F8.4,' * ',F7.4,/)

```

```

WRITE(N,37)      ((V1(I,J),J=3,4),(V3(I,K),K=4,6),I=1,2)
37 FORMAT(1H0,'VARIANCE-COVARIANCE MATRICES',2D16.5,10X,3D16.5,/1H ,
* T30,2D16.5,10X,3D16.5)
WRITE(N,38)      (V3(3,J),J=4,6)
38 FORMAT(1H ,70X,3D16.5)
WRITE (N,39) S1(10),S1(9),S3(10),S3(9)
39 FORMAT(1H0,'CONVERGENCE CODE, NO. OF ITERATIONS',5X,4F10.0)
WRITE(N,41) <
TOL#VAR%15<
41 FORMAT(// 'EVALUATION OF MAXIMUM LIKELIHOOD ESTIMATE RESULTS'/1H0,
* T20,'FIRST ASYMPTOTE',T53,'THIRD ASYMPTOTE',T81,'RETURN',/1H ,
* T ,8X,2('VALUE      MIN      MAX',10X),T79,'PERIOD,SEC',/)
XNPK#VAR%9<*VAR%10<
DO 50 I#1,22
XT#FLOAT%I-5</2
IF%1.EQ,22<XT#-ALOG%ALOG%XNPK/(XNPK-1.))
XE#EXP%-XT*SNGL%S3%3<<<
XB#%1.-XE</S3%3<
XC#%S3%4<-S3%1<<*XT*XE-S3%2<*XB/S3%3<
XA#XT/S1%2< **2
X1=DSQRT(S1%5< **2<XA*S1%6<< **2-2.*XA*V1%1,4<<
X3=DSQRT((S3(5)*XE)**2 + (S3(6)*XB)**2 + (S3(7)*XC)**2
* &2.*XE*XB*V3%1,5<&XB*XC*V3%2,6<&XE*XC*V3%1,6< <<
XS1=X1
XS3=X3
XF#S1%1<&XT/S1%2<
XG#XF-XS1*TOL
XH#XF&XS1*TOL
XI#XB*S3%2<&XE*S3%1<
XJ#XI-XS1*TOL
XK#XI&XS1*TOL
XL#1./%1.-EXP%-EXP%-XT<<</VAR%9<
WRITE(N,42) XT,XF,XG,XH,XI,XJ,XK,XL
42 FORMAT(1H ,F8.2,2X,3F10.4,3X,3F10.4,4X,1PE10.3<
50 CONTINUE
XM#%VAR%11<-XF</XS1
XN#%VAR%11<-XI</XS3
X0#NPK/VAR%9<
WRITE(N,51) VAR%11<,VAR%10<,X0,XM,XN
51 FORMAT(1H0,'OBSERVED PEAK',F7.4,2X,'IN',F6.1,' SEC',10X,'ESTIMATES
* BASED ON DATA FROM',F5.1,' SEC',9X,'STATISTICS =' ,2F7.2)
RETURN
END

```

NOMENCLATURE

a	Local speed of sound
D	General distortion factor
F	Cumulative probability function
f	Probability density function
f_c	Filter cutoff (-3 db) frequency
IDC	Circumferential distortion factor
IDL	Fan stall margin ratio
IDR	Radial distortion factor
KA2	Fan distortion factor
KRA	Radial distortion factor
KTH	Circumferential distortion factor
log	Natural logarithm
N	Number of extremes
N_0	Number of zero crossings, Eq. (13)
n	Number of independent samples
P	Pressure
R	Normalized autocorrelation function
r	Inlet duct radius
s	Estimated standard deviation
T	Return period, Eq. (10)
t	Reduced variate, Eq. (6), or time
x	General probability variate

y	General probability variate
α	General asymptote parameter
β	General asymptote parameter
Δt	Time interval
ϵ	Limiting distortion level, α/β
λ	Similarity parameter, Eq. (12)
ν	General asymptote modal parameter
σ	Standard deviation
Φ	Cumulative probability function

SUPERSCRIPT

\wedge	Estimate
----------	----------